NAVAL POSTGRADUATE SCHOOL

MONTEREY, CALIFORNIA

THESIS

FUEL INJECTION STRATEGY FOR A NEXT GENERATION PULSE DETONATION ENGINE

by

Tad J. Robbins

June 2006

Thesis Advisor:	Jose O. Sinibaldi
Second Reader:	Christopher M. Brophy

Approved for public release; distribution is unlimited

THIS PAGE INTENTIONALLY LEFT BLANK

REPORT DOCUMENTATION PAGE			Form Approved OMB No. 0704-0188
Public reporting burden for this collection of information is estimated to average 1 hour per response, including the time for reviewing instruction, searching existing data sources, gathering and maintaining the data needed, and completing and reviewing the collection of information. Send comments regarding this burden estimate or any other aspect of this collection of information, including suggestions for reducing this burden, to Washington headquarters Services, Directorate for Information Operations and Reports, 1215 Jefferson Davis Highway, Suite 1204, Arlington, VA 22202-4302, and to the Office of Management and Budget, Paperwork Reduction Project (0704-0188) Washington DC 20503.			
1. AGENCY USE ONLY ***(Leave blank)***	**2. REPORT DATE** June 2006	**3. REPORT TYPE AND DATES COVERED** Master's Thesis	
4. TITLE AND SUBTITLE: Fuel Injection Strategy for a Next Generation Pulse Detonation Engine		**5. FUNDING NUMBERS** N0001406WR20161	
6. AUTHOR(S) Tad J. Robbins			
7. PERFORMING ORGANIZATION NAME(S) AND ADDRESS(ES) Naval Postgraduate School Monterey, CA 93943-5000		**8. PERFORMING ORGANIZATION REPORT NUMBER**	
9. SPONSORING /MONITORING AGENCY NAME(S) AND ADDRESS(ES) Liberty Center 875 North Randolph Street, Suite 1425 Arlington, VA 22203-1995		**10. SPONSORING/MONITORING AGENCY REPORT NUMBER** N/A	
11. SUPPLEMENTARY NOTES The views expressed in this thesis are those of the author and do not reflect the official policy or position of the Department of Defense or the U.S. Government.			
12a. DISTRIBUTION / AVAILABILITY STATEMENT Approved for public release; distribution is unlimited		**12b. DISTRIBUTION CODE**	

13. ABSTRACT (maximum 200 words)

The Pulse Detonation Engine offers the Department of Defense a new low cost, light weight, and efficient solution to supersonic flight on many of its small airborne platforms. In the past, both liquid fuel and gaseous fuel designs have been partially developed and tested. Several aspects of these configurations have led to the need for the development of a new design, in particular the reduction of total pressure losses, and the removal of auxiliary oxygen system previously required to initiate a detonation wave in fuel-air mixtures within practical distances. Furthermore, higher repetition rates are required for practical thrust levels, as well as the use of liquid fuels, as these are more attractive due to their higher energy densities.

A new PDE configuration was designed to operate on the liquid fuel, JP-10. The fuel injection system was characterized using laser diagnostics so that the fuel injection strategy could be optimized for the specified operating conditions. The timing parameters for the fuel-air injection profile were characterized as well in order to deliver the desired amount and duration. This was a concurrent effort with computational simulations of the internal flow paths, design/integration of a novel transient plasma ignition system, and ongoing developments of a performance measurement test rig.

14. SUBJECT TERMS - Pulse Detonation Engine, PDE, Transient Plasma Ignition, TPI, Detonation, Deflagration, JP-10			**15. NUMBER OF PAGES** 79
			16. PRICE CODE
17. SECURITY CLASSIFICATION OF REPORT Unclassified	**18. SECURITY CLASSIFICATION OF THIS PAGE** Unclassified	**19. SECURITY CLASSIFICATION OF ABSTRACT** Unclassified	**20. LIMITATION OF ABSTRACT** UL

NSN 7540-01-280-5500 Standard Form 298 (Rev. 2-89)
Prescribed by ANSI Std. 239-18

THIS PAGE INTENTIONALLY LEFT BLANK

Approved for public release; distribution is unlimited

FUEL INJECTION STRATEGY FOR A NEXT GENERATION PULSE DETONATION ENGINE

Tad J. Robbins
Ensign, United States Navy
B.S., United States Naval Academy, 2005

Submitted in partial fulfillment of the
requirements for the degree of

MASTER OF SCIENCE IN MECHANICAL ENGINEERING

from the

NAVAL POSTGRADUATE SCHOOL
June 2006

Author: Tad J. Robbins

Approved by: Jose O. Sinibaldi
Thesis Advisor

Christopher M. Brophy
Second Reader

Anthony J. Healey
Chairman, Department of Mechanical & Astronautical Engineering

THIS PAGE INTENTIONALLY LEFT BLANK

ABSTRACT

The Pulse Detonation Engine offers the Department of Defense a new low cost, light weight, and efficient solution to supersonic flight on many of its small airborne platforms. In the past, both liquid fuel and gaseous fuel designs have been partially developed and tested. Several aspects of these configurations have led to the need for the development of a new design, in particular the reduction of total pressure losses, and the removal of auxiliary oxygen system previously required to initiate a detonation wave in fuel-air mixtures within practical distances. Furthermore, higher repetition rates are required for practical thrust levels, as well as the use of liquid fuels, as these are more attractive due to their higher energy densities.

A new PDE configuration was designed to operate on the liquid fuel, JP-10. The fuel injection system was characterized using laser diagnostics so that the fuel injection strategy could be optimized for the specified operating conditions. The timing parameters for the fuel-air injection profile were characterized as well in order to deliver the desired amount and duration. This was a concurrent effort with computational simulations of the internal flow paths, design/integration of a novel transient plasma ignition system, and ongoing developments of a performance measurement test rig.

THIS PAGE INTENTIONALLY LEFT BLANK

TABLE OF CONTENTS

LIST OF FIGURES

THIS PAGE INTENTIONALLY LEFT BLANK

LIST OF TABLES

THIS PAGE INTENTIONALLY LEFT BLANK

ACKNOWLEDGMENTS

First and foremost, I would like to thank my family and friends that have supported me in all my endeavors thus far in my life. Without their love and support, none of this would have been possible. I would also like to thank Professors Sinibaldi and Brophy for their support and guidance throughout this project. They truly made this a memorable and rewarding learning experience.

THIS PAGE INTENTIONALLY LEFT BLANK

I. INTRODUCTION

A. NEED FOR A PULSE DETONATION ENGINE

Pulse detonation engines (PDE) are a very attractive alternative for both subsonic and supersonic air-breathing propulsion applications. At this point many of the air-breathing vehicles and platforms make use of turbine engines. The turbine engine is designed around very complex and expensive machinery. Pulse detonation engines use the inherent physics of a detonation wave to produce high enthalpy products which are then accelerated to produce thrust. This immediately reduces the need for the turbo-machinery that many engines use today. The simplistic design of the PDE not only saves cost but potentially makes manufacturing very simplistic.

Pulse detonation engines have an inherent advantage of producing thrust without added machinery. The fuel-air mixture enters the combustion chamber and the fuel-air mixture is detonated. The detonation wave produced passes through the engine and produces a pressure difference behind the wave. This pressure wave produces thrust. If repeated at very high repetition rates, near constant thrust is produced. Unlike conventional rocket engines, which use constant pressure combustion, PDEs use a constant volume combustion process. This increases the thermodynamic efficiency from 36% of a conventional Brayton cycle, to about 55% for a detonation-based combustion cycle. This increase in efficiency coupled with the use of no moving machinery parts makes the PDE a sensible alternative for flight propulsion. Another attractive feature of this technology is that a cluster of PDEs can be used to achieve thrust vectoring by firing each PDE or a pair of PDEs at different times.

The lack of complex moving machinery makes the PDE a relatively low cost substitute for most air-breathing propulsion systems. Much of turbo-machinery is extremely expensive due to the complexity of design and precision needed. Pulse detonation engine technology is extremely simplistic and therefore, geometrical constraints are not as much of a concern. Pulse detonation propulsion systems are

expected to cost only about one-third of a comparable supersonic cruise capable propulsion system based on turbine technology. When discussing expendable platforms, this lower cost is extremely appealing.

Pulse detonation engines must operate at high frequencies, ideally greater than 40 Hz, in order to produce the minimum required thrust. At these high frequencies, the complete cycle must take place in a matter of milliseconds. This makes timing issues with respect to injection and ignition extremely critical. The sub-microsecond timing required to efficiently produce the detonation cycle calls for highly accurate and expensive fuel injectors and state of the art electronics. Operating at modest frequencies has historically required auxiliary oxygen in order to initiate the fuel-air mixtures. This excess oxygen system not only adds complexity but also decreases performance due to the added fuel products needed to produce thrust.

B. HISTORY OF PULSE DETONATION ENGINES AT NPS

Naval Postgraduate School (NPS) has been researching PDE technologies for several years. Two very distinct designs have been developed and tested throughout this research. A "pre-detonator" idea was first built and tested which takes a small amount of fuel and oxygen and detonates it before entering the main combustor, thereby using the highly energetic fuel-oxygen detonation to directly initiate a detonation wave within the fuel-air mixture inside the main combustor. A second idea makes use of Transient Plasma Ignition (TPI) to rapidly initiate a fuel-air mixture which subsequently accelerates the deflagration to detonation (DDT) process. This approach uses a volumetric electron discharge to rapidly initiate a fuel-air mixture.

The "pre-detonator" design was one of the first designs tested at NPS. This novel design took advantage of detonating a fuel-oxygen mixture in a very small volume. The detonation was then transmitted into the larger combustor, thus directly initiating a detonation wave in the larger fuel-air mixture. This engine design was able to achieve high repetition rates greater than 40 Hz which led to greater thrust. The disadvantage however of this design is that additional oxygen had to be used to pre-detonate the initial fuel-oxygen mixture. The additional system requirements that would have to be carried

on board to supply oxygen were deemed a penalty on the overall system. The auxiliary oxygen not only added an extra system to be carried on board, which adds weight and complexity, but it also resulted in performance losses. The specific impulse, which is defined as a ratio of thrust produced to fuel consumed, is decreased due to the added oxygen as shown in Equation (1). If this additional initiator can be eliminated, the specific impulse is greatly improved.

$$I_{sp} = \frac{F}{\dot{m}_{fuel}\, g} = \frac{F}{(\dot{m}_{fuel} + \dot{m}_{fuel\_init} + \dot{m}_{O_2})g} \tag{1}$$

A second design evaluated at NPS used a Transient Plasma Igniter to detonate a fuel-air mixture. The TPI technology has been developed and made efficient by Gundersen's team from the University of Southern California (USC) [2]. This technology makes use of a volumetric electronic discharge. Unlike a spark plug found in many internal combustion engines which use point sparks, the TPI produces a volumetric electron discharge via several streamers that originate at a charged electrode. This technology is very attractive because it is capable of replacing the need for added oxygen. At this point, however, high repetition rates have not been easily attained. The TPI research at USC has made many advances and the high repetition rates required by PDEs are expected to be achieved with the new engine design.

C. OBJECTIVES OF THESIS RESEARCH

The main objective for pulse detonation research is the development of a new PDE design. The developmental process is in conjunction with the thesis efforts of Hall [1], Holthaus [3], and Hutcheson [4]. The new PDE design will leverage on Holthaus's computational fluid dynamics (CFD) results of the internal flow of the fuel-air mixture, Hutchinson's experimental results on previous engine designs, and Hall's TPI integration design. The TPI technology will be integrated into this engine in order to eliminate the need for the auxiliary oxygen system. This engine was designed to encompass all of these parameters and achieve high repetition rates. The main focus of this thesis is the air flow and fuel flow delivery scheme coupled with optimization of the timing parameters. These two characteristics are extremely important.

THIS PAGE INTENTIONALLY LEFT BLANK

II. PULSE DETONATION THEORY

A. INTRODUCTION

Pulse detonation is not a new technology and can be traced back to the World War II era. The idea of using intermittent detonations to produce thrust can be traced back to Hoffman in Germany in the late 1930's [5]. Pulse detonation technology continues to emerge and high frequency repetitions are the focus of much research. Since each detonation wave produces thrust, this repetitive thrust production can be considered constant if the frequency rate of the detonation waves is driven high enough. Previous designs at NPS have focused on using gaseous fuels as well as auxiliary oxygen to facilitate detonation. The next generation PDE will operate on JP-10, a high energy-density liquid fuel. The auxiliary oxygen will be eliminated, thus increasing the specific impulse of the engine. The thermodynamic and cost benefits as compared to turbine powered engines make the PDE an attractive propulsion alternative for supersonic cruise missile applications.

B. DEFINITIONS OF TERMS

It is important to understand the difference between many similar terms associated with PDE theory [6].

Combustion – A rapid chemical process by which a gas, liquid, or solid fuel is rapidly oxidized resulting in a release of energy in the form of heat, and most often light. During this process the transformation of chemically bound energy into heat leads to a significant temperature rise.

Combustion wave – A propagating area of localized combustion. The wave consists of a heating zone ahead of the wave, a reaction zone, and an equilibrium zone.

Deflagration – A combustion wave that propagates at a subsonic velocity sustained by a chemical reaction that occurs at nearly constant pressure. The combustion process in rockets and gas turbines are examples of deflagration.

Explosion – An exothermic reaction where the rate at which energy is released exceeds the rate at which the surrounding environment can absorb that energy.

Detonation – A supersonic combustion event, in which the combustion wave formed, is composed of a strong shock sustained by the rapid energy release occurring in the highly compressed, high temperature region immediately behind the leading shock. The close coupling of the strong shock wave with the rapid combustion region is known as a detonation wave.

Deflagration and detonation are extremely different and the thermodynamic properties associated with each are shown in Table 1. A one-dimensional combustion wave is modeled in Figure 1. The associated thermo-fluid properties are shown and correspond with those referred to in Table 1.

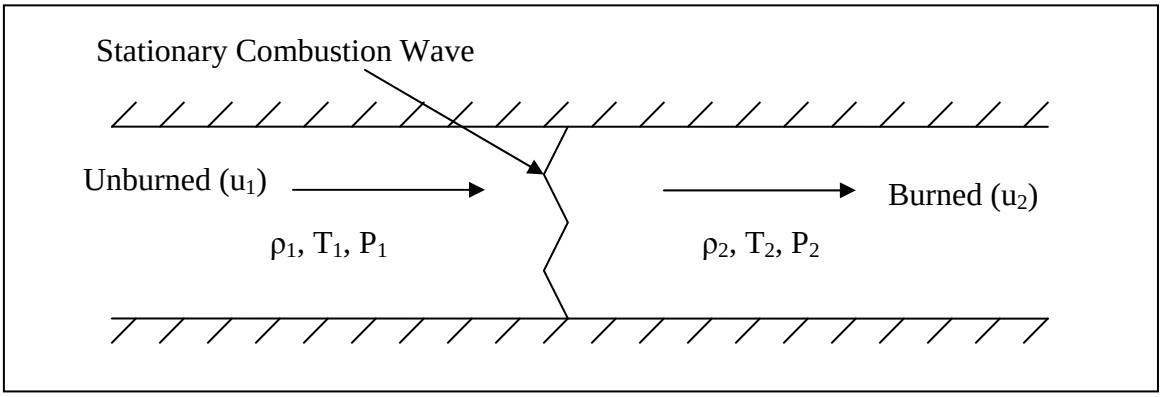

Figure 1. One-dimensional stationary combustion wave

Table 1. Qualitative differences between detonation and deflagration waves (After Ref. [7])

	Detonation	**Deflagration**
u_1/c_1	5-10	0.0001-0.03
u_2/u_1	0.4-0.7 (deceleration)	4-16
p_2/p_1	13-55 (compression)	0.98-0.976 (slight expansion)
T_2/T_1	8-21 (heat addition)	4-16 (heat addition)
ρ_2/ρ_1	1.4-2.6	0.06-0.25

C. ILLUSTRATION OF THE PDE CYCLE

1. PDE Cycle Characteristics

The PDE cycle is a relatively simple and efficient cycle. The PDE cycle takes advantage of constant volume combustion rather than the constant pressure combustion of its turbine counterparts. This gives the PDE a higher thermodynamic efficiency.

The cycle begins with the injection of an air-fuel mixture (1). The combustor tube of the engine fills with this mixture, purging any remaining products from the previous cycle (2). The air-fuel mixture then ignites (3). A detonation wave forms and travels through the engine to the exit (4) and (5). Rarefraction waves form and move back down the combustor tube (6) and (7). At this point the combustion products are purged (8) and the cycle repeats as shown in Figure 2.

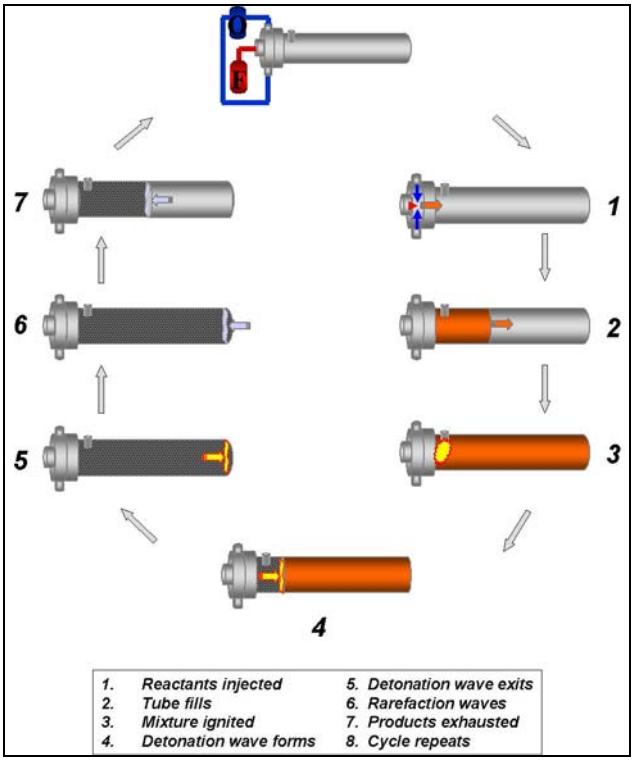

Figure 2. Pulse Detonation Cycle (From Ref. [8])

The cycle duration is on the order of milliseconds. Since the engine must operate at a high frequency to produce near constant thrust, the duration must be minimized. This is where the injection and ignition timing are important.

2. PDE Cycle Efficiency

Pulse detonation engines are considered to be more efficient than its jet engine counterparts. The advantages of the PDE can readily be understood by comparing its specific impulse (I_{sp}) to that of turbine based engines. Figure 3 shows how the specific impulse of the PDE compares to engines used on current platforms.

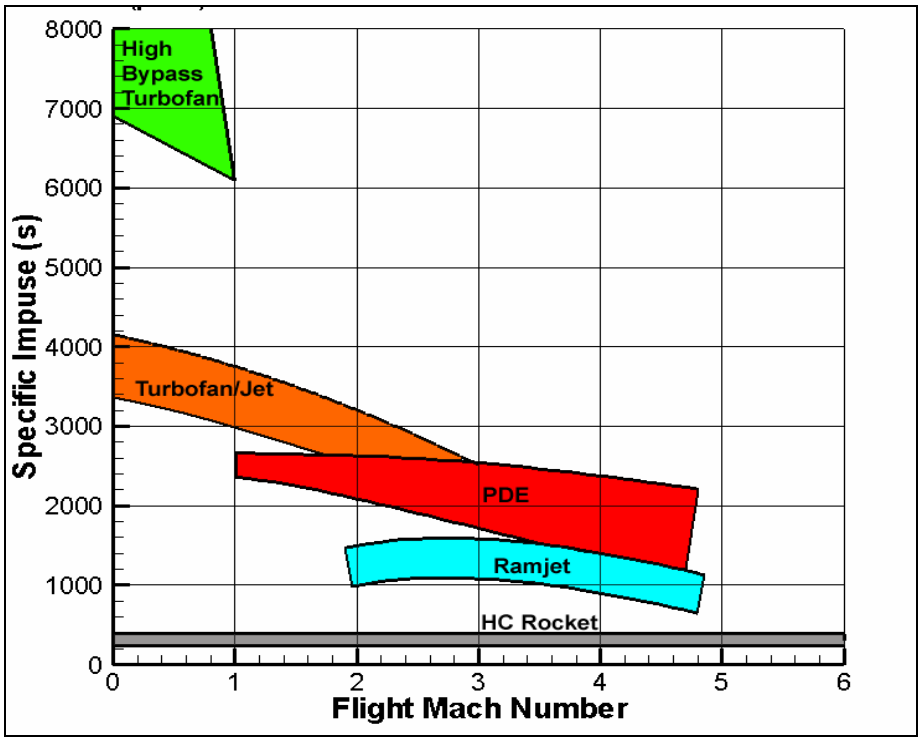

Figure 3. Comparison of specific impulse of various propulsion technologies (From Ref. [4])

The PDE is thermodynamically more efficient than most alternative systems in the Mach 2.5 – 5 flight range. Turbines make use of a constant pressure combustion process. This combustion process is deflagration, thus a subsonic flame front. The PDE, however, uses a detonation combustion process which can be approximated by a constant volume process. Therefore, the Brayton cycle can be used to analyze turbine engine thermodynamic efficiency and the Humphrey cycle can be used to model PDEs. A comparison of these two cycles can illustrate the increase in thermodynamic efficiency for PDEs. Figure 4 shows the pressure versus volume relationships as well as the temperature versus entropy relationships for both cycles. Work is transferred to and from the system by isentropic compression and expansion for both cycles. Heat addition in the Brayton cycle, steps 2-5, is replaced by Humphrey's steps 2-3, occurring at constant volume.

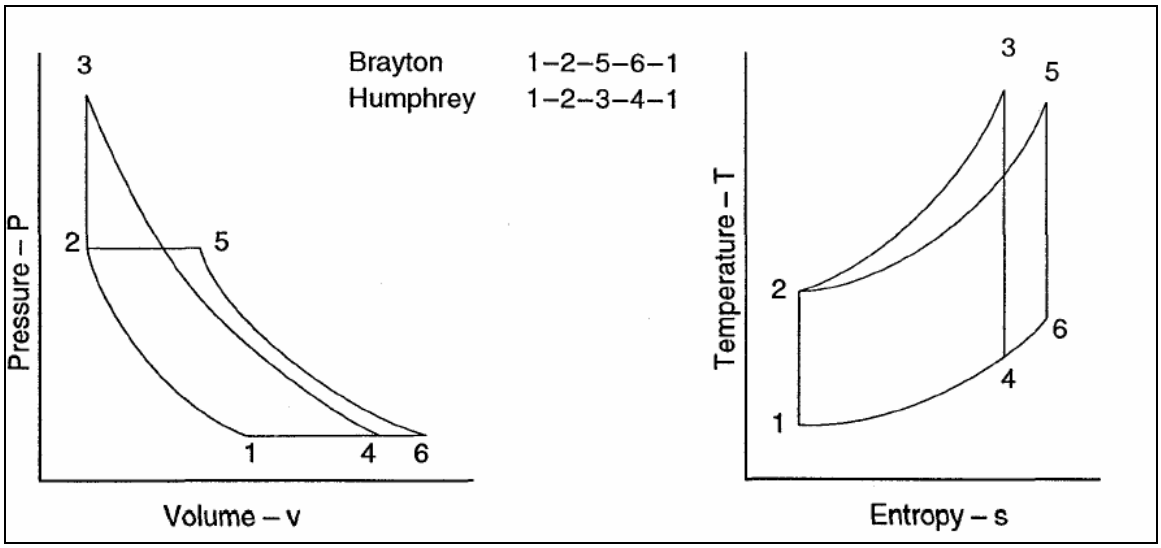

Figure 4. Pressure vs. Volume and Temperature vs. Entropy for Brayton and Humphrey Cycles (From Ref. [9])

Thermal efficiency (η) for a cycle can be defined as a ratio of the total work produced by a cycle to the total energy input. The efficiencies for each cycle are shown below in Equations (2) and (3).

$$\eta_{Brayton} = 1 - \frac{T_1}{T_2} \tag{2}$$

$$\eta_{Humphrey} = 1 - \gamma\left(\frac{T_1}{T_2}\right)\left[\frac{\left(\frac{T_3}{T_2}\right)^{\frac{1}{\gamma}} - 1}{\left(\frac{T_3}{T_2}\right) - 1}\right] \tag{3}$$

where γ is the specific heat ratio.

Plotting the thermal efficiencies for each cycle helps to illustrate the advantages of the PDE. Figure 5 shows a plot of the thermal efficiency of each cycle as a function of the pressure ratio, P_2/P_1. The Humphrey cycle is bounded by two specific heat ratios (γ). The upper limit is the γ for unburned reactants in a stoichiometric hydrogen/oxygen mixture. The lower limit is the γ for burned products in the reaction. The thermal efficiency gains of the Humphrey cycle over the Brayton cycle are approximately 20% over the range of compression ratios.

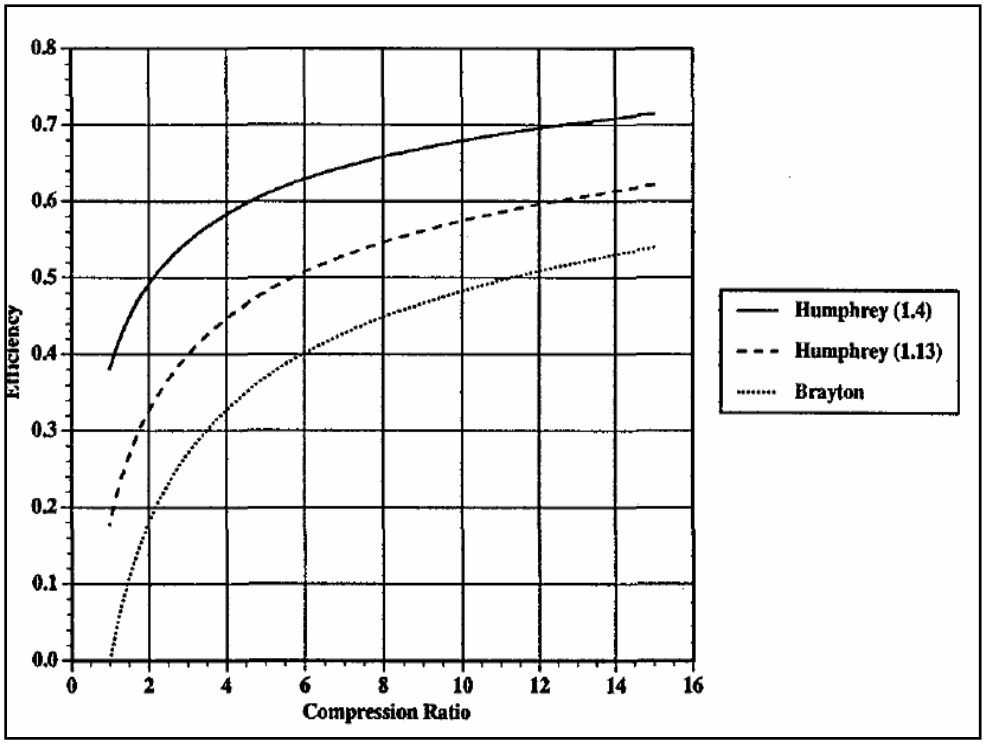

Figure 5. Thermal efficiency vs. Compression ratio for Humphrey and Brayton cycles (From Ref. [9])

III. DESIGN METHODOLOGY

A. OVERVIEW

A new engine was designed based on the aforementioned TPI technology. Much of the operational and testing equipment needed to test the new engine design is already in place at the NPS Rocket Lab. Inlet conditions to the PDE are simulated at the lab by using vitiated air. Hydrogen is burned with the air, along with make-up oxygen, to heat up the incoming air. This heated air is then delivered to the engine. Figure 6 shows a schematic of an engine setup at NPS. The vitiator implementation was achieved through several previous thesis efforts at NPS.

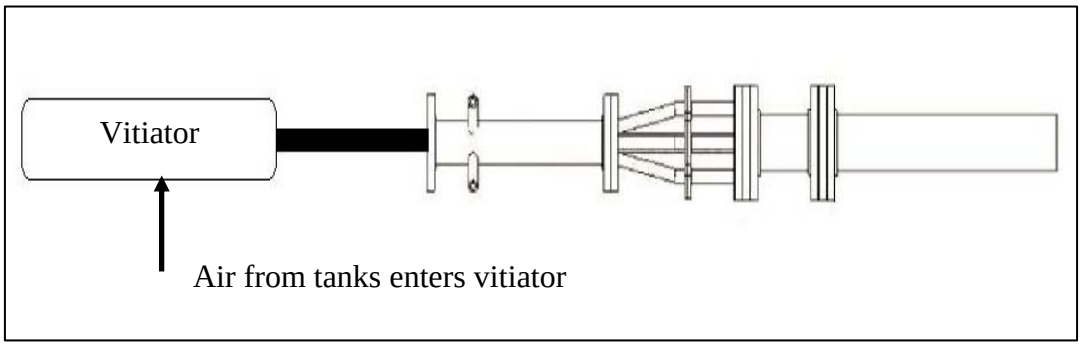

Figure 6. Vitiated air system schematic

Hall's TPI design has effectively eliminated the need for auxiliary oxygen [1]. In this design a split flow path was used to decrease velocities around the igniter. Previous TPI designs could not reach high flow rates due to quenching of the ignition event. This thesis work concentrated on efficiently splitting the flow but still remaining ergonomically compatible with both the current vitiator system and Hall's TPI design.

Timing issues are always a concern in PDE technology due to the high repetition rates required. While splitting the flow to two annuli efficiently was important, the fuel injection system was equally important. The fuel injectors were tested so that the timing parameters could be characterized. This allowed a timing sequence to be developed in order to reduce engine efficiency losses.

B. CHARACTERIZATION OF FUEL INJECTION SYSTEM

The fuel injection system is based around four liquid fuel injectors. These fuel injectors use hydraulic pressure to atomize and inject fuel to the system. Figure 7 illustrates a general schematic of how the system works. Fuel is fed to the injectors from a fuel tank which is pressure regulated with nitrogen. Pressurized hydraulic fluid is supplied to the injectors via a hydraulic pump. The hydraulic system is a recirculating system meaning that after the hydraulic fluid passes through the injector it returns to a reservoir which in turn supplies the pump.

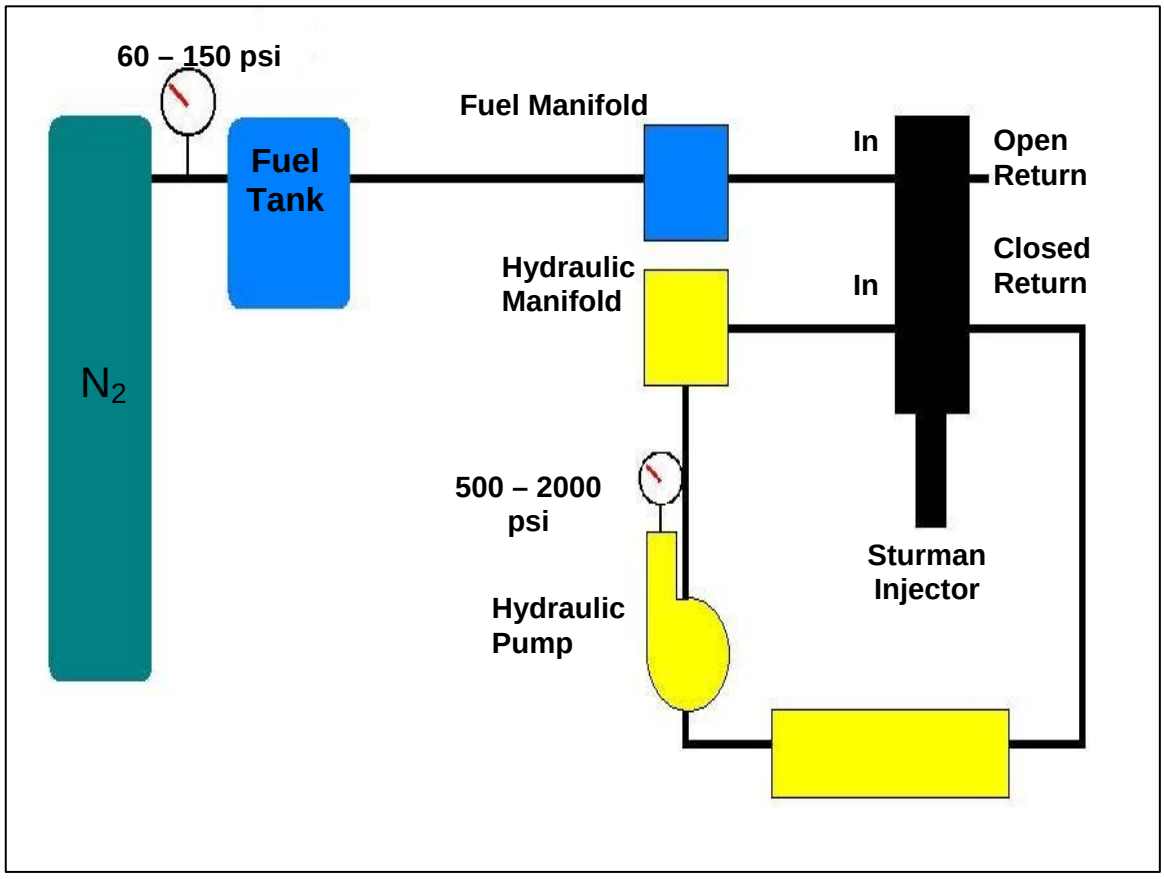

Figure 7. Fuel injection operating system schematic

The requirements for a liquid-fuel based detonation wave call for state of the art fuel injectors. Fuel droplets near the point of detonation must be on the order of three microns in size in order for the detonation wave to form. The fuel injectors used in this engine use hydraulic pressure to atomize the fuel droplets into sprays with characteristic Sauter Mean Diameters between twelve and twenty microns. The design of the fuel

injector tips amplify the hydraulic fluid and produce a pressure increase of approximately 10:1. In the testing, hydraulic pressures were varied from 500 psi to 2000 psi, thus the pressure within the injector ranged from 5000 psi to 20000 psi. This pressure increase forces the fuel out of a small orifice at the tip. The tip is comprised of two concentric annuli ten microns apart. The high pressure coupled with the small exit area effectively atomizes the fuel droplets to about twelve microns. The fuel droplets produced are not the required size, but if properly mixed with vitiated air, the fuel is vaporized almost completely. This combination permits a detonation wave to be generated.

1. Experimental Setup

Optical diagnostics were used to evaluate the parameters of each fuel injector. A laser was pointed at the fuel injection tip, and the scattering effects of the beam being attenuated through the spray were recorded by an oscilloscope via a Silcon based optical sensor. Figure 8 illustrates the diagnostic setup.

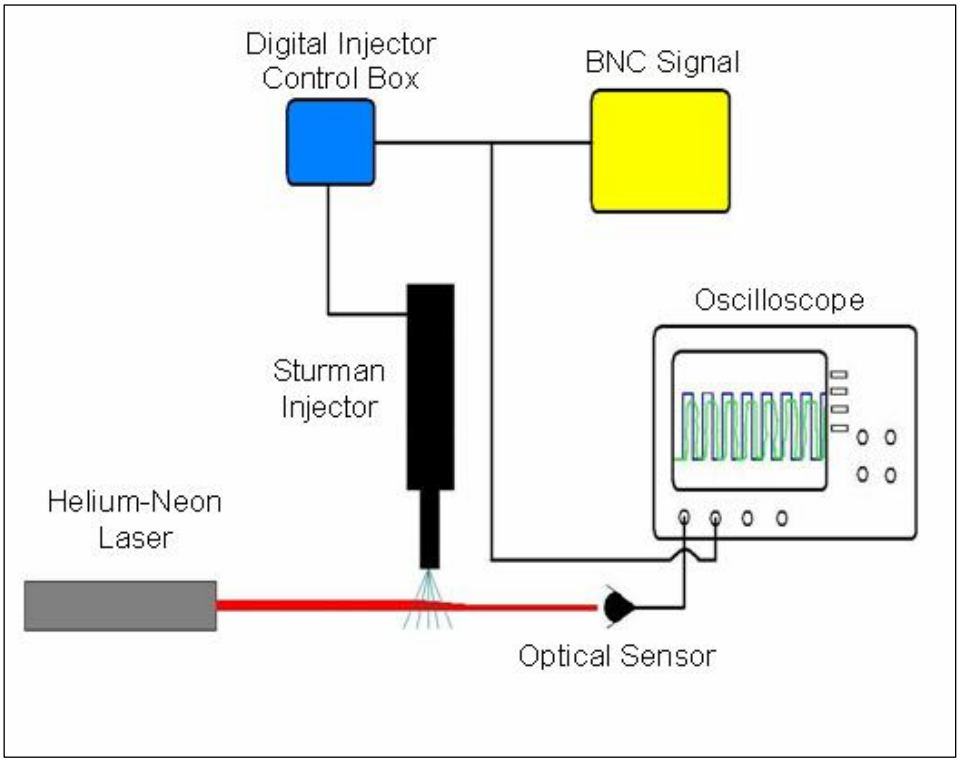

Figure 8. Electrical diagnostics schematic

A helium-neon (HeNe) laser was used in testing and operated at 633 nm. The laser beam cut through the spray and was detected by a 2 MHz Silicon based sensor. The fuel droplets scattered the light and thus the light intensity decreases. The detected signal

was then read into the *LeCroy LT374* 500 MHz oscilloscope. The control pulse from the pulse generator was also monitored with the oscilloscope as shown in Figure 8. This allowed the control pulse to be used to evaluate the injection pulse characteristics, specifically pulse width and pulse delay. All diagnostic equipment specifications can be found in Appendix A.

2. Post-processing Analysis

The input signal and output signal were analyzed with a program developed in MATLAB, found in Appendix B. The program took the input and output signals, shown in Figure 9, and calculated the injector pulse width and delay based on half altitude values.

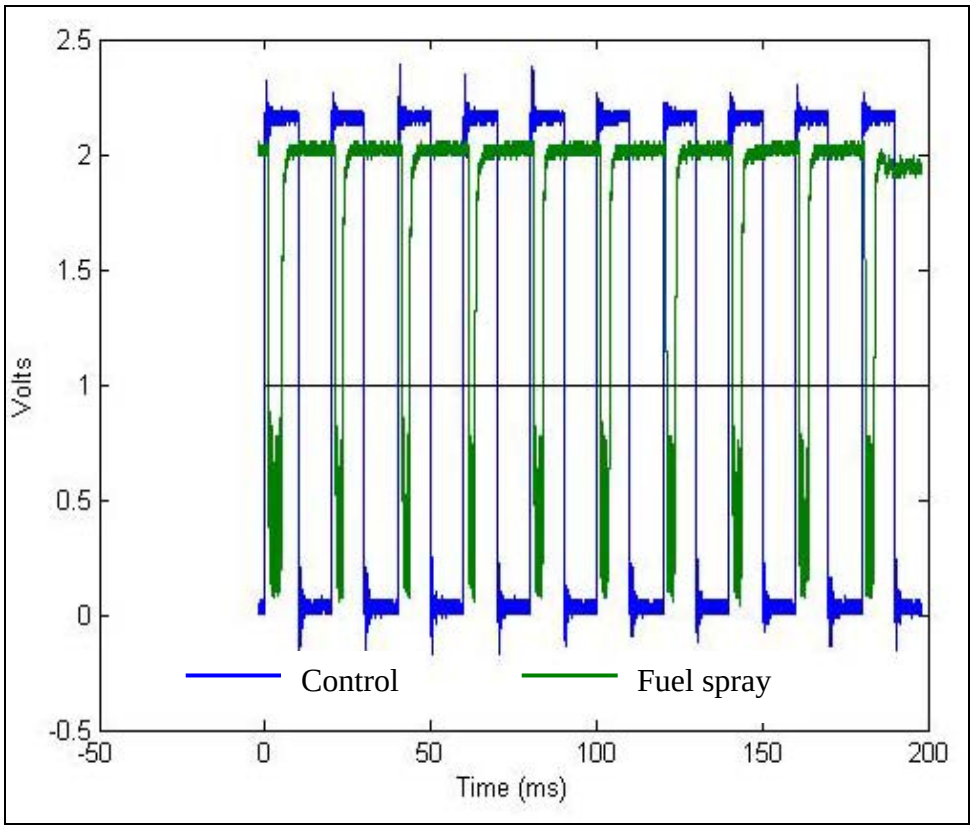

Figure 9. Control input signal plotted against injector output signal

A close up of the two signals, shown in Figure 10, helps illustrate what is meant by pulse width and pulse delay.

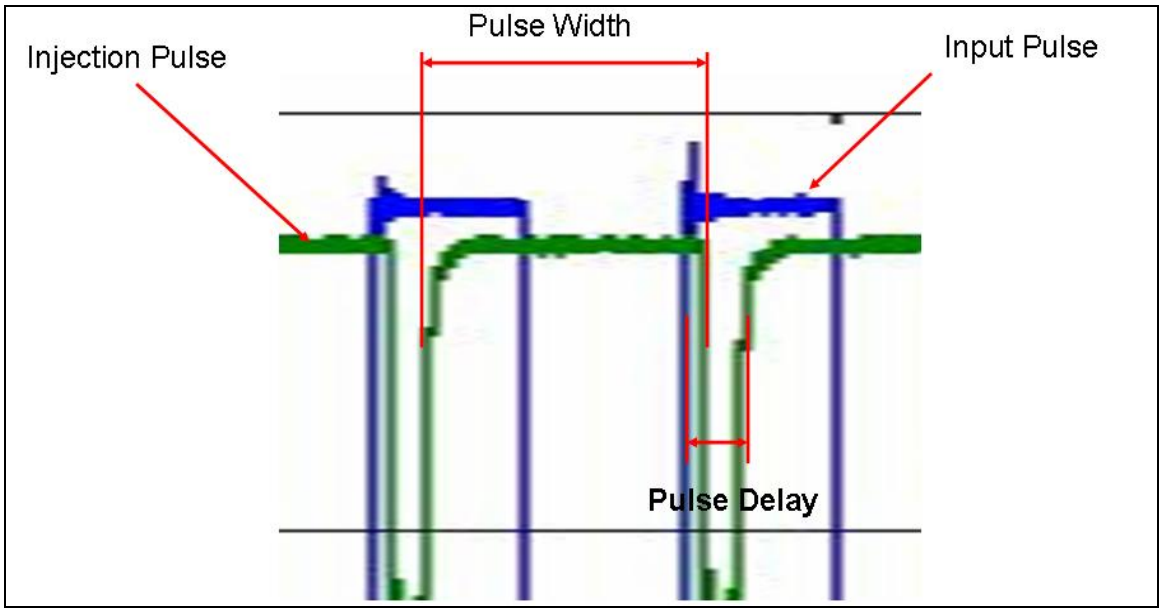

Figure 10. Signal characteristics, pulse delay and pulse width, shown on input and output signals

3. Typical Results

All four fuel injectors were characterized individually. The injectors were tested at 10 hertz for 1 second for each pressure setting. The hydraulic pressure was varied in 250 psi steps from 500 psi to 2000 psi. In general, the fuel injectors pulse width and pulse delay decreased with increasing hydraulic pressure. The four injectors all showed expected characteristics. Complete results will be discussed further in the next chapter.

C. GEOMETRICAL DESIGN CONSIDERATIONS

Several geometrical considerations were involved in the design of the new PDE. This thesis focuses on the design of the engine fuel-air mixture delivery system and its interface to the engine head flange, all which resides upstream of the TPI. Hall concentrated his efforts on the design and integration of the TPI system. Compatibility concerns were addressed in the design. As shown in Figure 11, the TPI design makes use of flow not only on the outside of the TPI but flow through an inside annulus as well.

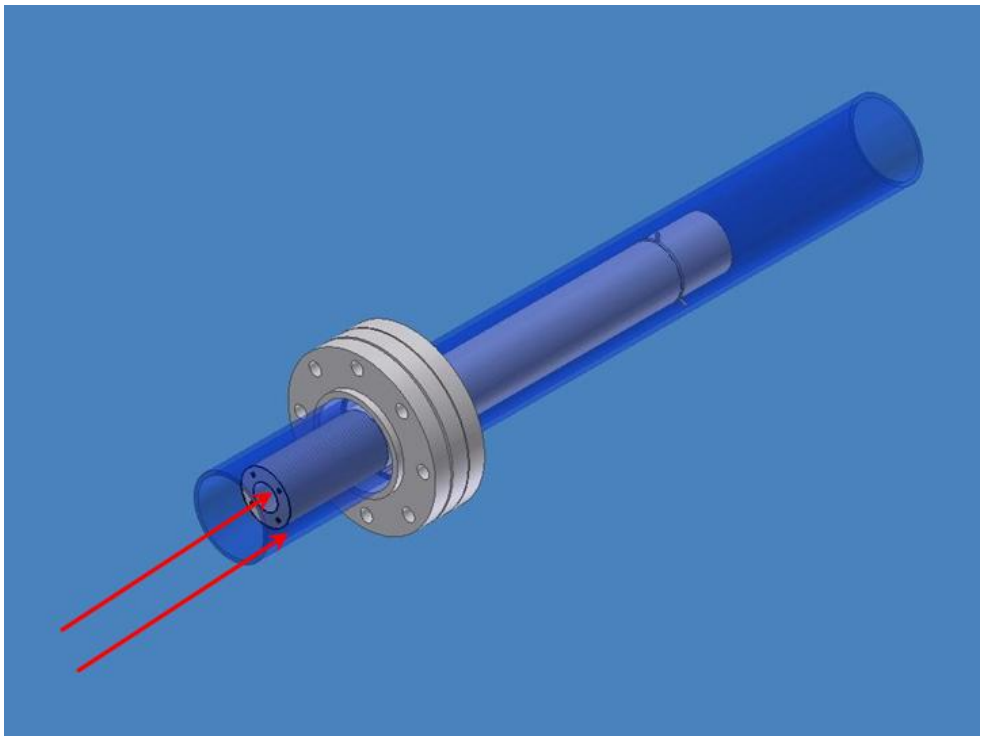

Figure 11. Transient Plasma Ignition Design (From Ref. [1])

1. Split Flow Design

The flow ratios in each annulus will change, so the design must account for this flexibility. Space is very limited at the entrance point of the TPI design. A similar configuration previously used by Hartsfield [10] was used to turn the flow into the outer annulus. The flow is taken into an outer plate and turned inside the flange using two consecutive, but opposite in direction, forty-five degree turns as shown in Figure 12. This design was a joint development with Hall.

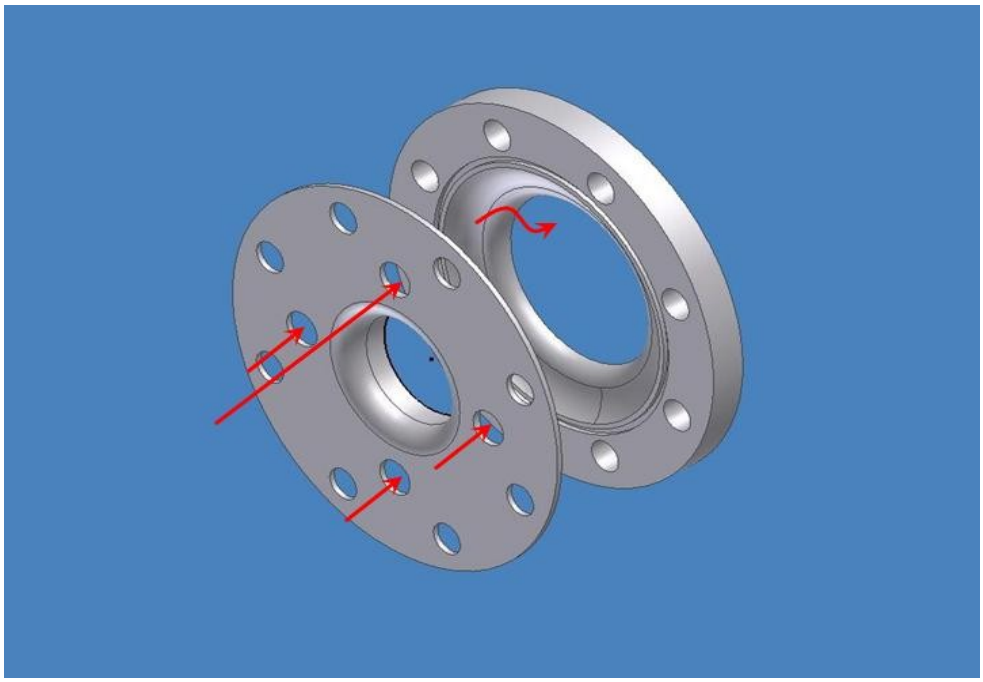

Figure 12. Outer flow turning flange

Four pipes bring flow into the turning flange. These are welded to the turning flange outer plate, making this one piece. This assembly can be seen in Figure 13.

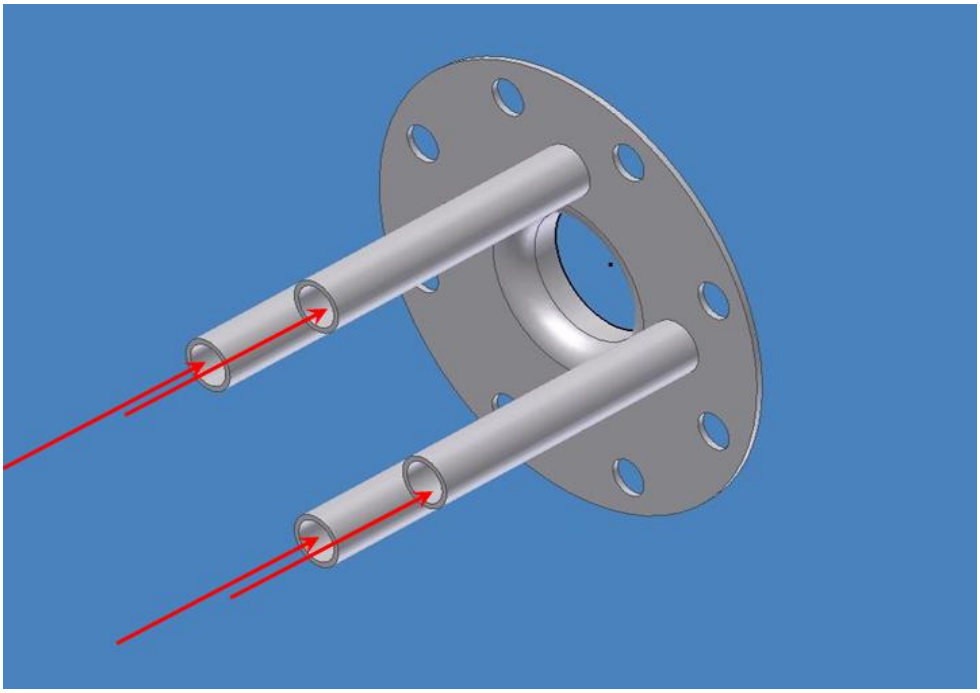

Figure 13. Outer flow turning flange assembly

This assembly is then connected to the upstream section of the engine via four flanges. In order to mate all pieces between the head flange of the TPI section and the fuel injection section of the engine, these flanges had to be machined down due to the space constraints. Figure 14 provides a three-dimensional view of the flanges.

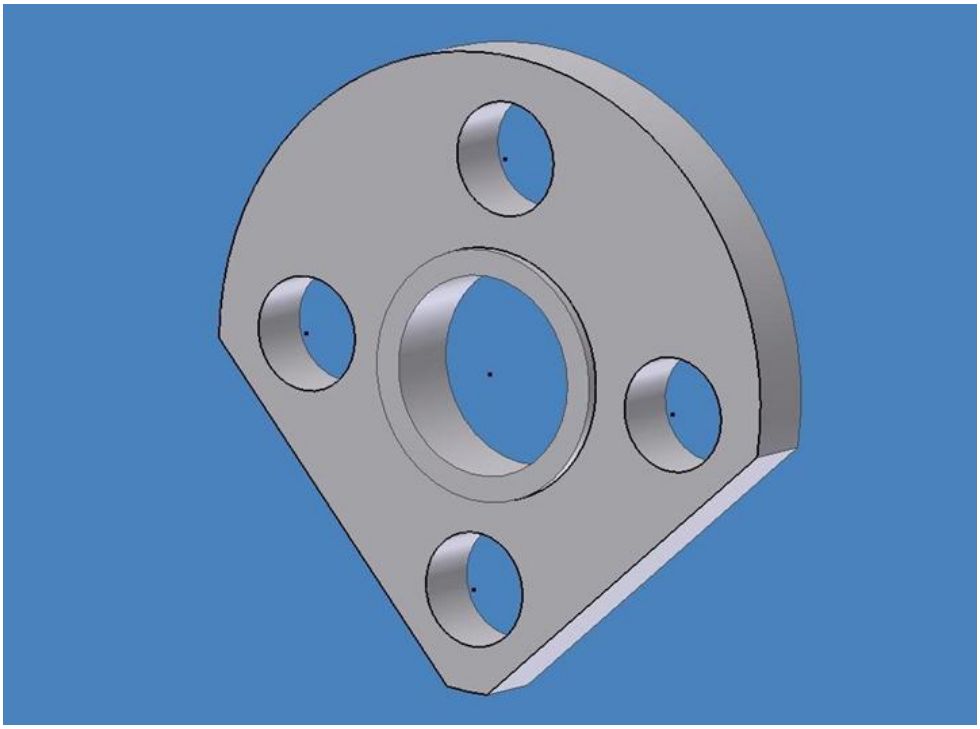

Figure 14. Outer pipe flange

The outer pipes mate up to four duplicate flanges on the upstream side. On the upstream side, the flange have a recess in them in order to accept various chokes to control mass flow over the outer section of the TPI section. The choke design will be discussed further in a later section. Figure 15 illustrates how the choke and the flange are assembled.

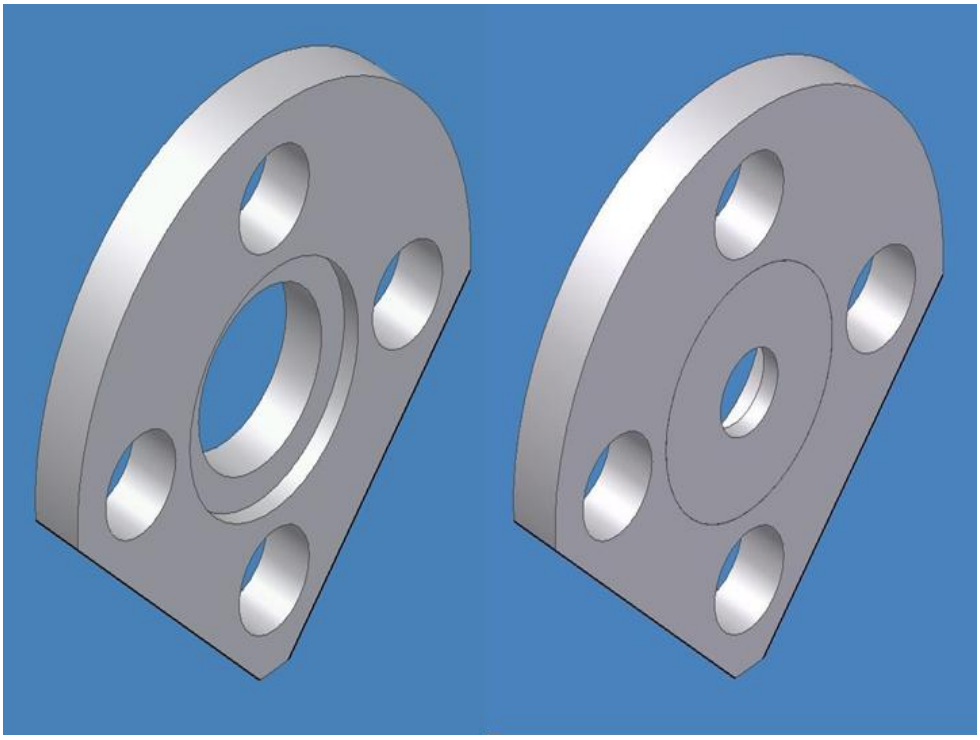

Figure 15. Upstream flange for outer flow shown with and without choke

The outer fuel-air mixture reaches the four previously mentioned flanges via a spider-like assembly of four pipes. This feature of the current design was needed in order to move the flow outward in the radial direction so that accessibility and maintenance were not hindered. These four pipes are permanently fixed to a flange that splits the flow to these outer four pipes and a center pipe. The center pipe is also fixed to this flange. This assembly is shown in Figure 16.

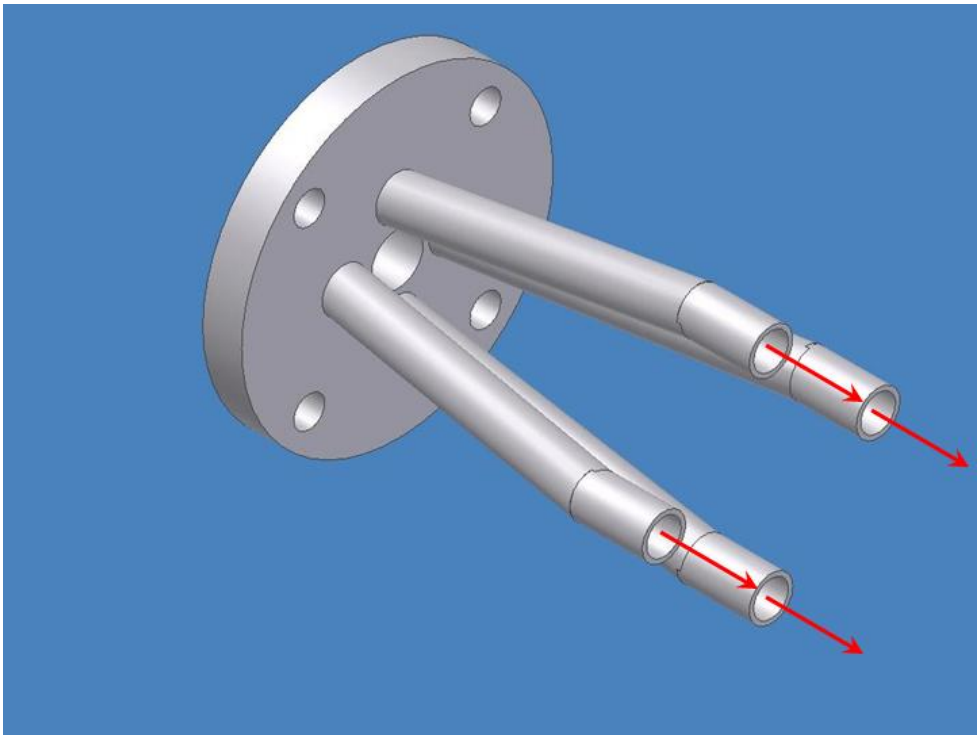

Figure 16. Split flange assembly

The flow through the center annulus of the TPI was also addressed. There was not enough space to mount a pipe with a complete flange. Mounting tabs were used on the aforementioned center pipe to overcome this problem. Figure 17 shows the pipe that carries the fuel-air mixture into the center annulus.

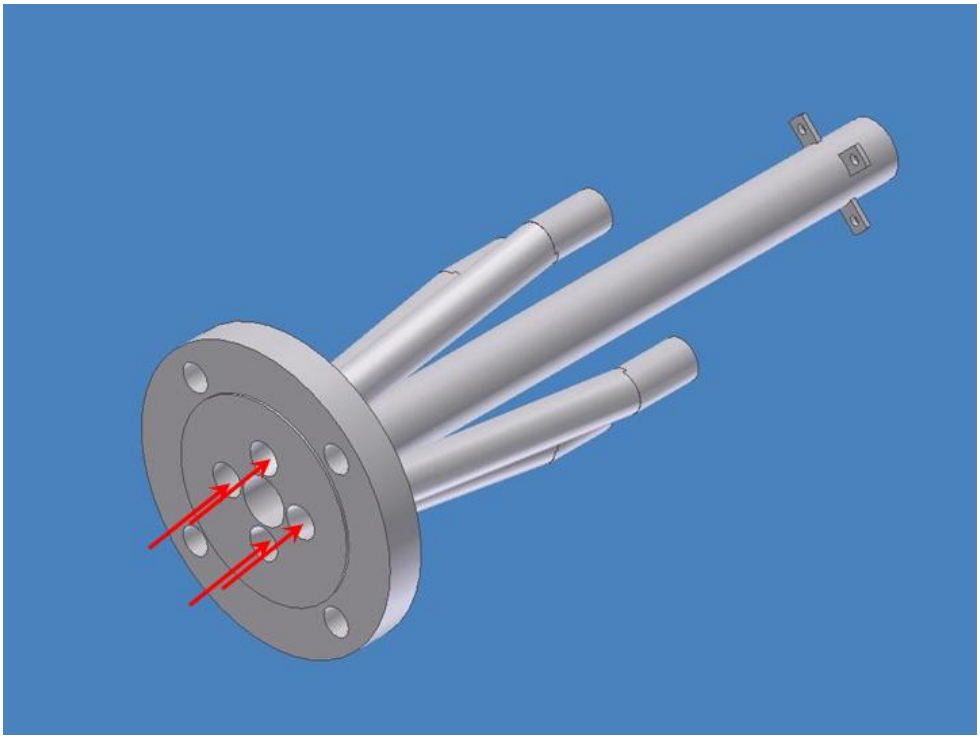

Figure 17. Center flow pipe

2. Fuel Injection Design

Upstream of the split flange is where both fuel and air are injected. Vitiated air comes in through the same path as previous designs [11]. A single injection point for the fuel was required as supported from the preliminary results obtained during the fuel characterization. The injection tube was designed to not only mate up with the vitiated air inlet, but also to have the fuel injected all at one point. The previous design had fuel injected in four separate arms. The current design of the injection tube assembly is shown in Figure 18. This assembly shows the flange on each side. In the upstream section we see the flange that meets up with the vitiated air output flange and in the downstream section we see the flange where the flow was split.

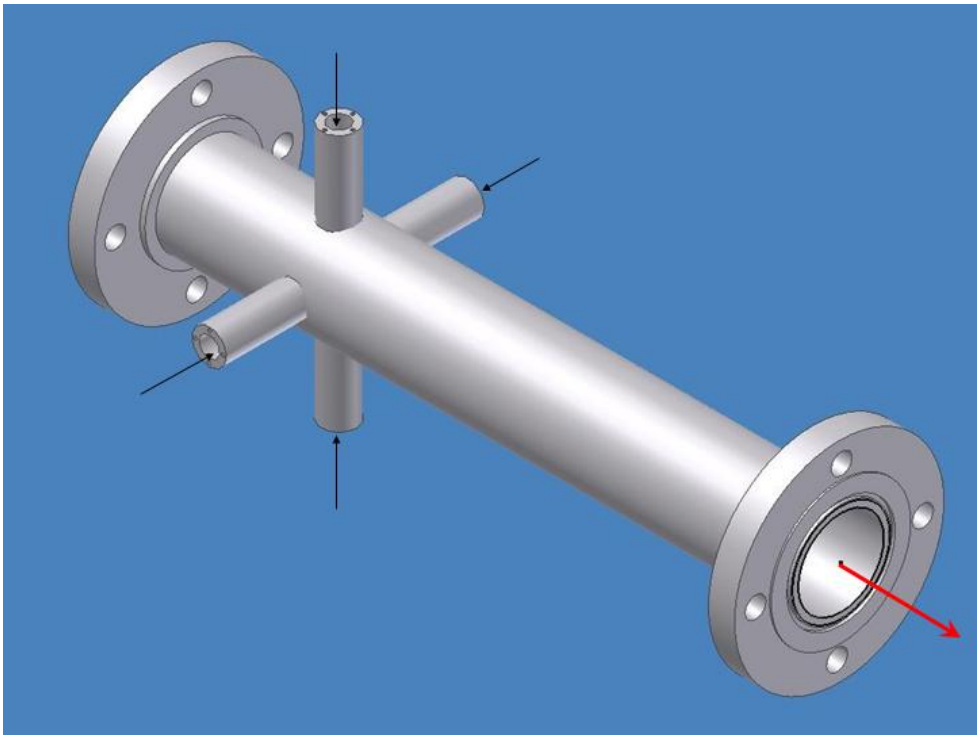

Figure 18. Injection tube assembly

At the end of the injection tube is the location where the split flange is attached. The flow is actually split at the end of the injection tube via a split cone. This split cone helps to split the flow with minimal pressure losses and recirculation zones. This cone was designed to incorporate a choke for the center tube. The downstream side of the cone has a recess in order to accept the various chokes that control the mass flow through the center annulus of the TPI. Figure 19 illustrates the split cone and the choke assembly and the complete engine assembly is shown in Figure 20.

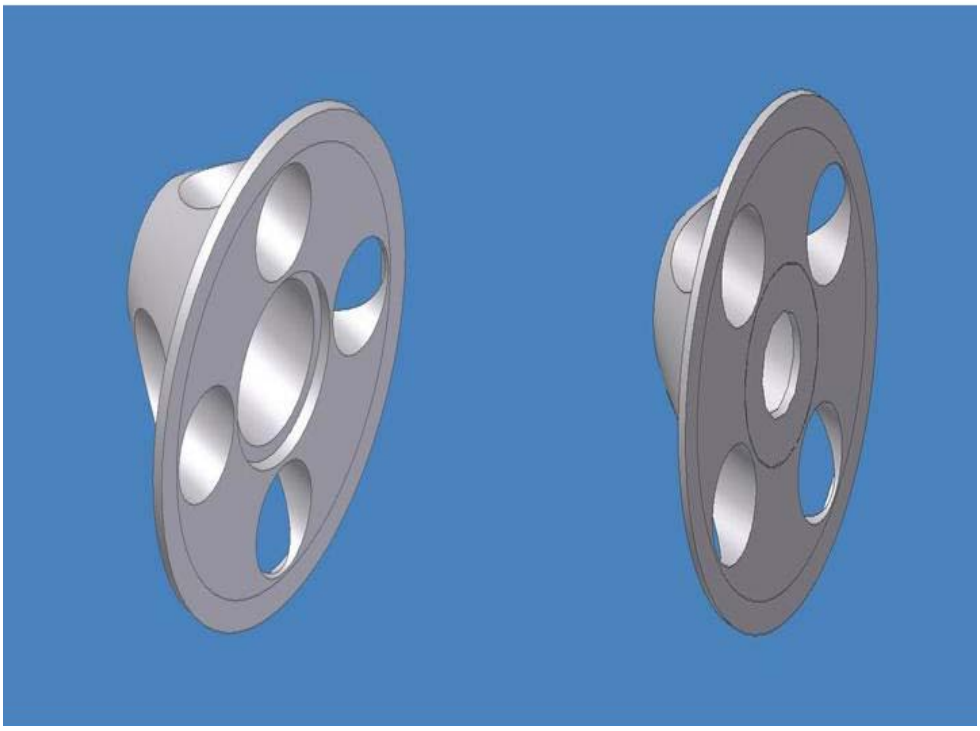

Figure 19. Split cone with and without choke assembly

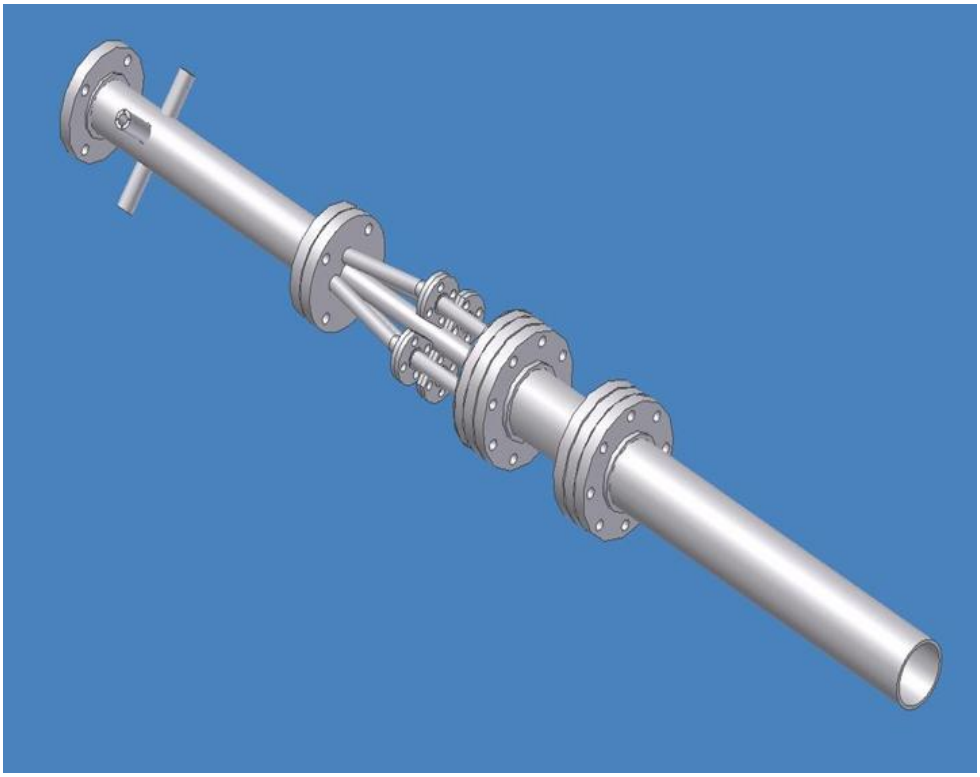

Figure 20. Next generation Pulse Detonation Engine

D. FUEL-AIR MIXTURE TIMING PARAMETERS

1. Fuel-air Mixture Properties

The fuel injection characterization and the data taken on the previous engine design were used to evaluate the timing parameters of the new engine design. This was done to improve ignition times and flow rates. The continuity equation, Equation (4) was used to calculate the time steps of the fuel-air mixture throughout the engine.

$$\dot{m} = \rho V A_C \tag{4}$$

Initially, the basic equation for the JP-10 and air combustion is used, Equation (5).

$$C_{10}H_{16} + 14(O_2 + 3.76N_2) = 10CO_2 + 8H_2O + 52.64N_2 \tag{5}$$

From this reaction equation, the stoichiometric fuel-air ratio can be found using the molar masses of the fuel and air, Equation (6).

$$\frac{F}{A} = \frac{10 \cdot MM_C + 16 \cdot MM_H}{14 \cdot MM_{O_2} + 52.64 \cdot MM_{N_2}} \tag{6}$$

Once the fuel-air ratio was calculated, the equivalence ratio can be determined using Equation (7). This is a ratio of an actual fuel-air ratio to the stoichiometric ratio. Different equivalence ratios determine whether the engine is running lean, $\varphi < 1$ (more air than stoichiometric) or rich $\varphi > 1$ (more fuel than stoichiometric).

$$\varphi = \frac{F/A_{Actual}}{F/A_{Stoich}} \tag{7}$$

Initially, air flow rates were going to be determined based on expected fuel flow rates. Fuel injectors were thought to have an injection volume of 130 mm^3/stroke. However, after obtaining real-time equivalence measurements from the previous engine design [4], it was determined the equivalence ratios would be determined based on the desired air flow rates. Using the desired equivalence ratio and the desired air flow rate, the fuel mass flow rate can be found from Equation (8).

$$\frac{F}{A} = \frac{\dot{m}_{Fuel}}{\dot{m}_{Air}} \tag{8}$$

The total mass flow rate of the fuel-air mixture can be calculated from Equation (9) once both fuel flow rate and air flow rate are determined.

$$\dot{m}_{Total} = \dot{m}_{Fuel} + \dot{m}_{Air} \tag{9}$$

Since air is a compressible fluid, the density is a function of pressure and temperature. Varying choke designs require varying pressures, thus we must assume density is a variable property as shown in Equation (10).

$$\rho = \frac{P}{RT} \tag{10}$$

Since a fuel-air mixture is flowing through the engine, the density of the mixture must be determined. This found by combining the densities of the fuel and the air as shown in Equation (11).

$$\rho_{Mix} = \frac{\dot{m}_{fuel}\ \rho_{fuel} + \dot{m}_{Air}\ \rho_{Air}}{\dot{m}_{fuel} + \dot{m}_{Air}} \tag{11}$$

Now that all the fluid properties are determined, the timing characteristics of the fuel-air mixture can be determined. Based on the cross-sectional properties and lengths of the engine sections in question, the fuel-air timing can be determined using Equations (12), (13), and (14).

$$t = \frac{L}{V} \tag{12}$$

$$V = \frac{\dot{m}_{Total}}{\rho_{Mix} A} \tag{13}$$

$$t = \frac{L \rho_{Mix} A}{\dot{m}_{Total}} \tag{14}$$

2. Choke Design

Chokes were designed for both the outer flow and the center flow. Holthaus' work [3] indicated that a 50% split of the mass flow was optimal for the flow characteristics likely to be observed in the PDE design. Therefore, chokes were designed to divert 50% of the flow to the inside and 50% of the flow to the outside flow path. The choke design was a function of the pressure ratios needed to achieve the desired air flow rates. Three chokes were designed for three different flow rates for both the inner and outer flow. Given a desired air flow rate, the diameter of the choke opening was found using Equations (15) and (16).

$$\dot{m}_{Air} = \frac{A_{Choke} P_{Upstream} \Gamma_{Air} \mathrm{K}_{Air}}{T^{.5}} \tag{15}$$

$$A_{Choke} = \frac{\pi}{4} d_{Choke}^2 \tag{16}$$

3. Fuel Injection Schemes

Two fuel injection schemes were considered. Parallel fuel injection was the primary strategy studied. With parallel injection, clusters of one, two, or four injectors would be fired. For a low desired total flow rate, only one injector would be fired. At a slightly higher flow rate, two injectors would be fired. Likewise, at even higher flow rates, four injectors would be fired. In this case, air mass flow rates of 0.25 kg/s, 0.5 kg/s, and 1.0 kg/s were studied with one, two, and four injectors fired respectively.

Time sequential injection, or series injection, was also studied. Series injection is derived from parallel injection. For the detonation cycle to take place, the combustion tube must be completely filled with reactive products. In the case where the combustion tube may not completely fill with parallel injection, series injection must be used. Series injection is essentially a parallel injection scheme taking place one after another making the fuel-air mixture "plug" longer. The primary concern was the two slowest flow rates. In the slowest case, one injector would be fired after another until the fuel-air mixture plug length completely fills the combustion tube. At the middle flow rate, a cluster of two injectors would be fired after another.

IV. RESULTS

A. FUEL INJECTOR CHARACTERIZATION

1. Input Characteristics

The fuel injector input signal was delivered via a pulse generator in the control. A BNC pulse generator was used to send a 20 Hz signal to the injector digital control electronics which then sent the electric pulse to the injector being tested. A total of ten pulses were sent to each injector on each run. The output of the BNC pulse generator was monitored on the oscilloscope and compared to the fuel pulse as it came out of the injector. A sample of the BNC pulse is shown in Figure 21.

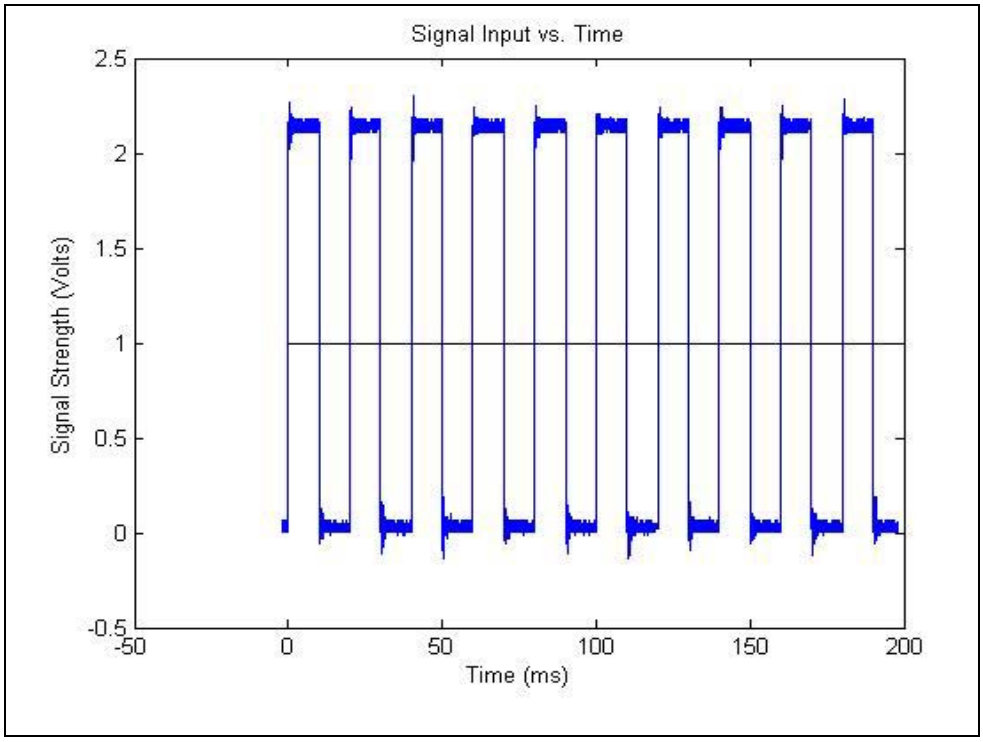

Figure 21. Input signal to fuel injector

2. Output Characteristics

All four injectors were tested individually. The hydraulic pressure was varied between 500 and 2000 psi in 250 psi increments. The pressure was varied so that a proper engine operating pressure could be determined. A typical output can be shown

plotted against the input signal in Figure 22. The HeNe laser path to the optical sensor was scattered by the fuel droplets when the fuel was flowing, thus a decrease in signal.

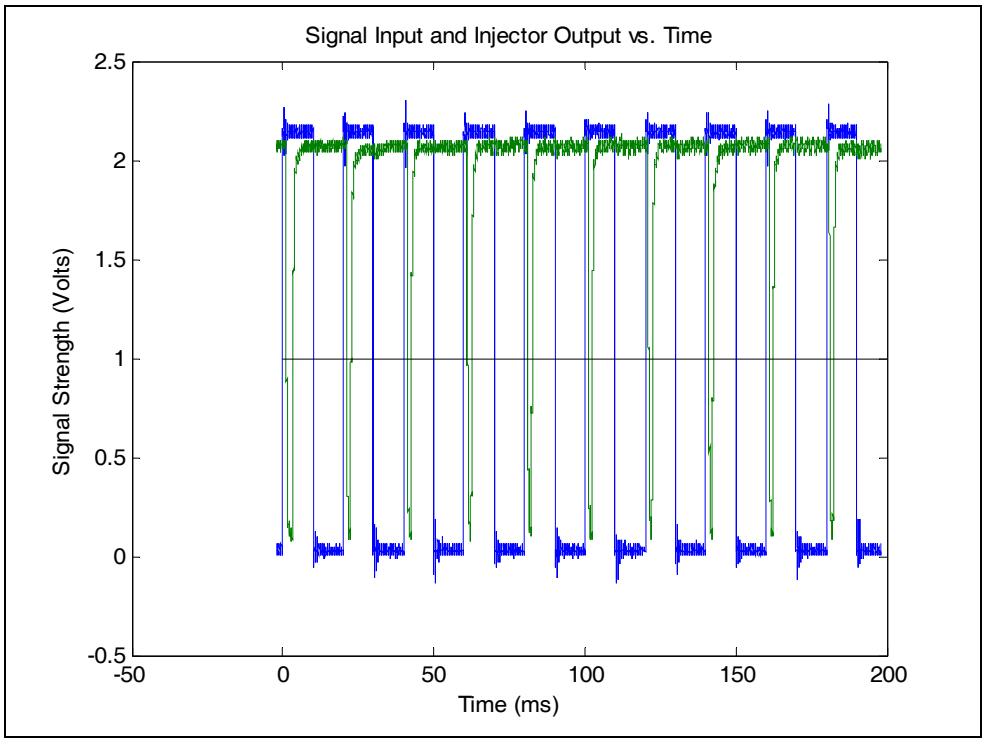

Figure 22. Typical injector output plotted against signal input

Three sets of data were taken for each pressure on each injector. All three sets of data were averaged using two different approaches to find the average pulse width and pulse delay. The first average was a simple average of all data. The second average, the one used for analysis, eliminated outlying data that tended to skew true averages. For the most part, these were the first or first and second pulses on each trial. At least the first pulse on each run was extremely different than the rest of the pulses. The standard deviations for the second averages are quite a bit less than for the first averages. Below, Table 2 shows the second averages for pulse delay for all four injectors over the array of hydraulic pressures. To better show the general trend for the pulse delay of these four injectors, this data was shown graphically in Figure 23.

Table 2. Pulse delay data for fuel injector characterization

Delay (ms) PSI							
Injector	**500**	**750**	**1000**	**1250**	**1500**	**1750**	**2000**
1	na	1.0259	0.9228	0.8965	0.8596	0.8444	0.8315
2	1.349	1.3149	1.2004	1.1656	1.1224	1.1183	1.1351
3	1.2693	1.0998	0.962	0.9281	0.9031	0.8944	0.8727
4	2.0559	1.0701	0.9539	0.9048	0.8802	na	0.8288

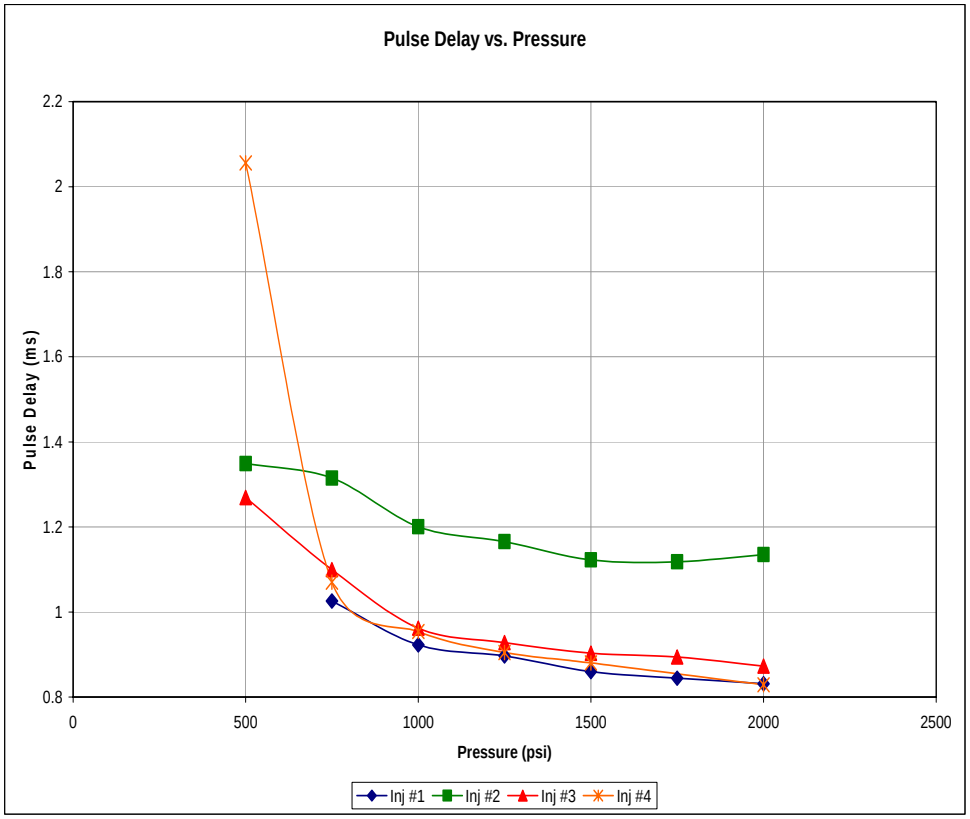

Figure 23. Pulse delay vs. hydraulic pressure

Pulse width for each injector is shown in Table 3. Figure 24 shows this data graphically.

Table 3. Pulse width data for fuel injector characterization

Pulse Width (ms) PSI							
Injector	**500**	**750**	**1000**	**1250**	**1500**	**1750**	**2000**
1	na	2.7808	2.0716	1.8029	1.6436	1.5352	1.4332
2	3.5415	2.1594	1.7798	1.5315	1.4073	1.3612	1.3244
3	4.1383	2.6906	2.051	1.8975	1.7423	1.6529	1.5774
4	2.4762	2.2049	1.6838	1.5522	1.3474	na	1.2348

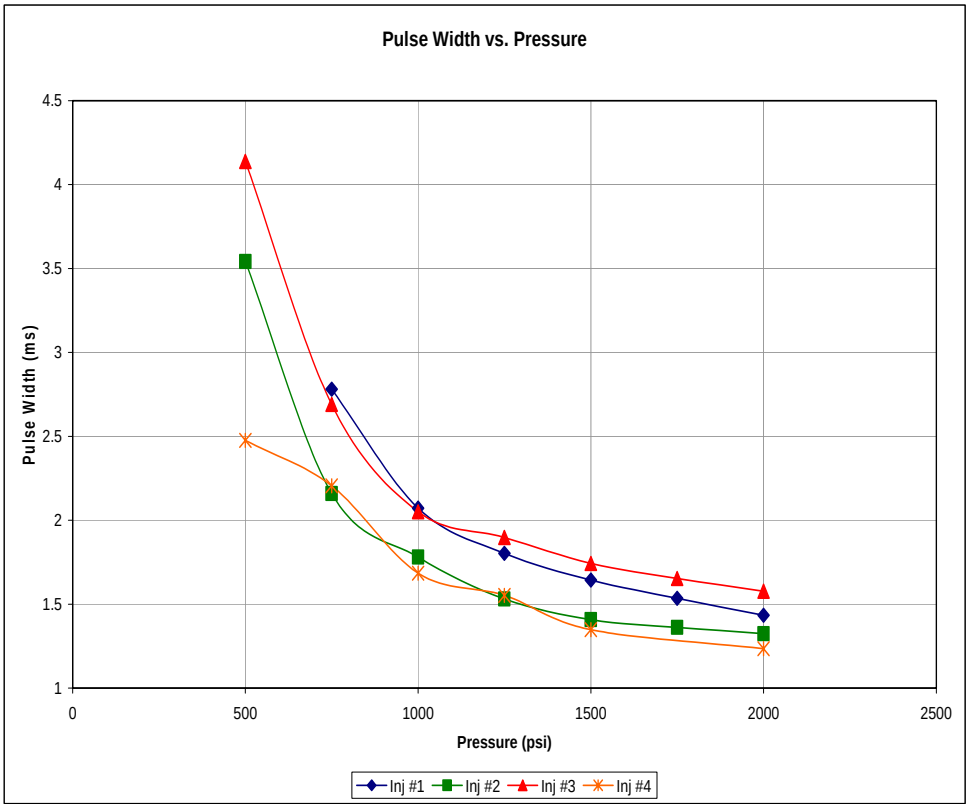

Figure 24. Pulse width vs. hydraulic pressure

After this data was compiled and analyzed, the hydraulic pressure of 750 psi was chosen to be the appropriate operating pressure for engine testing. A 5 millisecond (ms) pulse delay was desired. This is the time previously found to be optimal for the detonation cycle. The output at 500 psi was too sporadic to be a viable operating pressure, making 750 psi the required operating parameter. At this pressure, 5 ms was not achievable. With the implement of fuel injection time scheming, the correct operating parameters for the PDE could be achieved.

B. FUEL/AIR PLUG TIMING

1. Initial Calculations

Initially, the stoichiometric equation for the combustion of JP-10 was analyzed and several reaction properties were calculated. The fuel-air ratio at the given equivalence ratio, density of fuel-air mixture at various pressures, and the gas constant for the mixture were all calculated. All of these values are used to evaluate other properties of the PDE cycle. A summary of the supplementary values can be found in Table 4.

Table 4. Fuel-air mixture properties

$Mdot_{air}$ (kg/s)	**ρ_{Mix} (kg/m^3) upstream**	**ρ_{Mix} (kg/m^3) downstream**
0.25	1.59875	0.79938
0.5	1.99711	0.99855
1	3.04878	1.52439
R=271.833 J / kg/K		**F/A=.0780435**

Concurrently, the previous engine design was tested with the injectors to compile data as a guide for ignition parameters for the next generation PDE. NPS collaborated with Stanford University to determine the real-time equivalence ratio of the fuel-air mixture using advanced IR laser based absorption spectroscopic diagnostics. Also, pressure measurements were taken at different points in the PDE for varying mass flow rates [4]. An equivalence ratio of 1.1 was determined to be optimal for engine performance. In addition to these measurements, the injection pulse width for the cluster of four injectors was determined to be 5 ms downstream. This is different than when the injectors were characterized. The difference is most likely due to recirculation zones throughout the engine and possible fuel-wall impingement effects. A summary of the local pressure and temperature data taken for various air mass flow rates is shown in Table 5 [4].

Table 5. Pressure data with varying air mass flow rates in old NPS PDE (From Ref. [4])

$mdot_{air}$ (kg/s)	**P (kPa)**	**T (F)**
0.4	119.3	400
0.5	129.6	400
0.65	144.8	400
0.8	161.3	400
0.9	181.3	400
1.1	214.4	400
1.3	260.6	400

Pressure data had to be interpolated from the above data since additional air mass flow rates were desired. Also, the pressures provided are all points downstream of all choke conditions. It was approximated that the pressure conditions upstream of the choking condition were twice that of the downstream condition. Table 6 shows the interpolated pressure data points, denoted as P1, including the upstream pressure data points, denoted as P2. The downstream pressure is lower because the flow is choked thus producing a normal shock which results in a total pressure loss.

Table 6. Pressure data points for desired air mass flow rates

mdot (kg/s)	**P2 (Pa)**	**P2 (psia)**	**P1 (Pa)**	**P1 (psia)**	**T (K)**
0.25	103766	15.05	207532	30.1	477.444
0.5	129621	18.8	259243	37.6	477.444
1	197880	28.7	395759	57.4	477.444

The chokes for the mass flow could then be designed with the pressure data in Table 6. The chokes are necessary so that flow rates through the inside and outside annuli of the TPI can be controlled. The choke diameters were determined using Equations (15) and (16) based on the aforementioned 50% flow split to the inner and outer annuli. At the point of choking, each of the four outer pipes see 12.5% of the total mass flow rate. Likewise, the center pipe sees 50% of the total mass flow rate. Tables 7

and 8 show the required diameters of the small chokes and the large choke, respectively. These choke diameters will set up the corresponding pressures shown above, thus properly dividing the flow to each annulus of the TPI.

Table 7. Required choke diameters for outer flowpath

$Mdot_{air}$ (kg/s, per tube)	**d (in)**	**d (m)**
0.03125	0.3557	0.009035
0.0625	0.447	0.01135
0.125	0.5161	0.01311

Table 8. Required choke diameters for center flowpath

mdot (kg/s)	**d (in)**	**d (m)**
0.125	0.712	0.01808
0.25	0.8939	0.02271
0.5	1.033	0.02624

Using the equivalence ratio of 1.1 and Equations (7) and (8), the mass flow rate for the fuel injectors was found. As discussed earlier, the fuel flow rate from the injectors was not exactly known. With the fuel flow rate known and the desired air flow rates, a total mass flow rate was found for each injection scheme discussed earlier. Table 9 displays the desired air mass flow rates, and total mass flow rates for the three parallel configurations, all at the desired equivalence ratio of 1.1.

Table 9. Total mass flow rates for various parallel injection configurations

	1 Injector	**2 Injectors**	**4 Injectors**
$mdot_{JP10}$ (kg/s)	0.01951	0.039022	0.078044
$mdot_{air}$ (kg/s)	0.25	0.5	1
$mdot_{total}$ (kg/s)	0.26951	0.539022	1.078044

2. Timing Characteristics

Using the Equations (12), (13), and (14), the timing characteristics for the engine were determined. As fuel is injected into the engine, it mixes with the vitiated air. Since the fuel is injected over a period of 5 ms, a fuel-air "plug" is created. The time difference between the leading edge of the plug and the trailing edge of the plug can be assumed to

be 5 ms. Thus, only the timing characteristics for the head end were calculated. Times were calculated at three different points in the engine. Figure 25 illustrates the three points at which times were calculated.

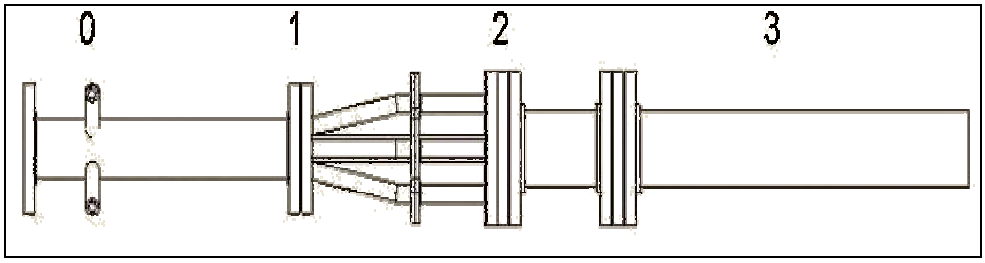

Figure 25. Timing characteristic locations

Point 1 in the illustration above denotes the location at which the fuel-air mixture reaches the flow splitting cone. Point 1a, not depicted above, represents the locations at which both the center and outer flows reach their respective choke points. For the center flow, this coexists with point 1. For the outer flow, the choking point is at the flanges seen between point 1 and point 2. Point 2 is the point at which the flow enters the combustor tube and thus the outer flow reaches the transient plasma ignition region and the center flow enters the inner annulus. Point 3 indicates the point at which the center flow and outer flow merge.

Initially, parallel injection scheming were characterized. In this scheme, injectors were fired in clusters of one, two, or four. This allows for the varying air mass flow rates. Table 10 shows the calculated time values for the head end of the fuel-air plug at the various locations. The values denoted with a prime notation (x') depict all of the time characteristics of the flow diverted through the center. All time values are in seconds.

Table 10. Timing characteristics for parallel injection

$mdot_{air}$ (kg/s)	**t1 (s)**	**t1a' (s)**	**t2' (s)**	**t3' (s)**	**t1a (s)**	**t2 (s)**	**t3 (s)**
0.25	0.01294	0.01294	0.01472	0.02421	0.01707	0.01849	0.03509
0.5	0.00808	0.00808	0.00920	0.01512	0.01066	0.01155	0.02192
1	0.00617	0.00617	0.00702	0.01154	0.008136	0.009027	0.01694

Due to the fact that the combustion tube may not be completely filled, series injection was modeled. Table 11 shows the calculated fuel-air plug lengths for the parallel injection schemes described previously. The same notation as above applies where the prime notated numbers (x') represent the flow through the center. The point of this study is to determine if the combustion tube completely fills with the fuel-air mixture. If this does not occur, series injection must be used. The combustion tube is approximately 1 m in length.

Table 11. Fuel-air plug length in combustion tube

$mdot_{air}$ (kg/s)	**L_{plug}' (m)**	**L_{plug} (m)**	**Injectors fired**
0.25	0.8317	0.4753	1
0.5	1.3316	0.7609	2

It is important to note that an overlap must be used to ensure the equivalence ratio doesn't decrease. Based on the individual injector characteristics found in Appendix C, an overlap of approximately 100 μs should be used.

THIS PAGE INTENTIONALLY LEFT BLANK

V. CONCLUSIONS

A. CONCLUSIONS

1. Fuel Injection and Timing Characterization

Fuel injectors were characterized, resulting in a selection of an optimal operating parameter for PDE operation: hydraulic pressure of 750 psi and fuel pressure greater than 100 psi. The individual characteristics of each fuel injector showed that individual control for each injector was needed and that it was also deemed necessary to develop a fuel injection strategy.

Two fuel injection schemes were analyzed; parallel and serial injection. At low flow rates (mdot_air < 0.25 kg/s), a serial injection scheme is recommended (one injector a time with a slight overlap of 100 μs). At large air flow rates (mdot_air > 1.0 kg/s) the parallel injection scheme is recommended (all 4 injections at the same time). For moderate mass flow rates, a combination of serial and parallel injection is recommended (2 injectors in parallel followed by the other 2 injectors in parallel with 100 μs overlap.)

2. Engine Design

The transient plasma ignition was successfully integrated into the new design. Modeling proved that single point injection was required which was achieved through the injection tube design. Challenges in splitting the flow were also addressed and accomplished through the use of a flow split cone to efficiently split the flow to the inner and outer annulus. Also the outer flow turning flange was an important design to efficiently deliver the outer fuel-air mixture from a four-pipe configuration into an annulus but keeping the flow inline with the outer annulus in a quick and smooth manner. Choke design also was of equal importance so that the flow for both annuli can accurately be choked in order to set up the correct mass flow rates throughout the engine.

B. FUTURE WORK AND SUGGESTIONS

1. Test Rig

The engine is currently undergoing fabrication and construction. Future work will include assembling the engine and developing a test matrix. A testing sequence can be

derived from past models. The data acquisition and control panel are the same as in previous testing at NPS. Essentially, little needs to be done to develop the test rig.

2. Vary Mass Flow Rates

The study for the engine designed in this thesis is based on only three different air mass flow rates. After these initial mass flow rates, with their respective fuel injection schemes, are tested, different mass flow rates should be tested. Higher mass flow rates should always be the goal because higher mass flow rates produce higher repetition rates which will produce greater thrust.

3. CFD Study of Fuel Injection Schemes

A CFD study might be useful to study the fuel injection, especially at the lowest mass. At the two larger flow rates, the fuel injection is symmetric, that is opposing fuel injectors are fired. At the lowest flow rate, only one injector is fired. This may cause an unwanted problem in the mixing of the fuel and vitiated air. Although higher flow rates are the desired end state, this would be a very valuable study.

APPENDIX A. ELECTRICAL DIAGNOSTIC EQUIPMENT SPECIFICATIONS

OSCILLOSCOPE

Model Number	**LT374**
Vertical System	
Input Channels	4
Analog Bandwidth @ 50 Ohms (-3 dB)	500 MHz
Hardware Bandwidth Limits	20 MHz, 200 MHz
Input Impedance	50 Ohms ± 1%; 10 MOhms / 12 pF typical (using PP006 probe)
Input Coupling	1 MOhms : AC, DC, GND; 50 Ohms : DC, GND
Maximum Input	50 Ohms : 5 Vrms; 1 MOhms : 400 Vmax (peak AC <=5 kHz + DC)
Vertical Resolution	8 bits; up to 11 bits with enhanced resolution (ERES)
Sensitivity (50 ohm or 1 M ohm)	2 mV - 10V/div fully variable
DC Gain Accuracy	± (1.5% + 0.5% of full scale)
Offset Accuracy (50 ohm or 1 M ohm)	± (1.5% + 0.5% of full scale + 1 mV)
Offset Range	2 mV – 99 mV/div: ± 1 mV 100 mV – 99 mV/div: ± 10 V 1V – 10 V/div: ±100 V
Isolation Channel-to-Channel	> 250:1 at same V/div settings

Timebase System

Timebases	Main and up to four independent zoom traces simultaneously	
Ranges	500 ps/div – 1000 s/div	1 ns/div – 1000 s/div
Clock Accuracy	<=10 ppm	
Interpolator Resolution	5 ps	
External Clock Frequency	500 MHz maximum, 50 Ohms, or 1 MOhms impedance	
Roll Mode – Operating Range	time/div 500 ms – 1000 s/div or sample rate < 100 kS/s max	
External Timebase Clock	500 MHz maximum external sample clock input on front panel EXT BNC	

Acquisition System

Single-Shot Sample Rate	
1 Channel Max.	4 GS/s
2 Channels Max.	4 GS/s
3 – 4 Channels Max.	2 GS/s
Maximum Acquisition Points/Ch	
1 Channel Max.	500k / 2M / 8M
2 Channel Max.	500k / 2M / 8M
3 - 4 Channel Max.	250k / 1M / 4M

Acquisition Modes

Random Interleaved	50 GS/s for repetitive signals: 200 ps/div – 1 µs/div

Sampling (RIS)

Single-Shot	For transient and repetitive signals: 1 ns/div – 1000 s/div
Sequence	
LT262 / 264	2 – 400 segments
LT372 / 374	2 – 1000 segments
Memory Option M or L	2 – 400 segments
Intersegment Time	50 µsec max.

Acquisition Processing

Averaging	Summed averaging to 10 sweeps; continuous averaging with weighting range from 1:1 to 1:1023 (standard). Summoned averaging up to 10 6 sweeps (optional with WAVA)
Enhanced Resolution (ERES)	From 8.5 to 11 bits vertical resolution
Envelope (Extrema)	Envelope, floor, roof for up to 10 6 sweeps

Triggering System

Modes	Normal, Auto, Single, and Stop
Sources	Any input channel, external, Ext/10 or line; slope, level, and coupling unique to each source (except line trigger) Inactive channels usable as trigger inputs.
Slope	Positive, Negative, Window
Coupling modes	DC, AC, HF, HFREJ, LFREJ
AC Cutoff Frequency	7.5 Hz Typical
HFREJ, LFREJ	50 kHz typical
Pre-trigger delay	0 – 100% of horizontal time scale

Post-trigger delay	0 – 10000 divisions
Hold-off by time or events	Up to 20s or from 1 to 99 999 999 events
Internal trigger range	±5 div
Max trigger frequency	500 MHz (350 MHz on LT264, LT262)
External trigger input range	±0.5 (±2.5 V with Ext/5 selected)
Maximum ext. input @ 50 Ohms	±5 V DC or 5Vrms
Maximum ext. input @ 1 MOhms	400 Vmax (DC + peak AC < 5 kHz)

Automatic setup

Auto Setup	Automatically sets timebase, trigger, and sensitivity to display a wide range of repetitive signals
Vertical Find	Automatically sets the vertical sensitivity and offset for the selected channels to display a waveform with maximum dynamic range

Probes

Model PP006	10 : 1, 10 MOhms with auto-detect (one per channel)
Probe System: Probus®	Automatically detects and supports a wide variety of differential amplifiers; active, high-voltage, current, and differential probes
Scale Factors	Up to 12 automatically or manually selected

Color Waveform Display

Type	VGA color 8.4" flat-panel TFT-LCD
Resolution	VGA 640 x 480 pixels

Screen Saver	Display blanks after 10 minutes (when screen saver is “on”)
Real Time Clock	Date, hours, minutes, and seconds displayed with waveform
Number of Traces	Display a maximum of eight traces. Simultaneously display channel, zoom, memory, and math traces.
Grid Styles	Single, Dual, Quad, Octal, XY, Single + XY, Dual + XY; Full Screen gives enlarged view of each style.
Intensity Controls	Separate intensity control for grids and waveforms
Waveform Styles	Sample dots joined or dots only — regular or bold sample point highlighting.
Trace Overlap Display	Select opaque or transparent mode with automatic waveform overlap management.

Analog Persistence Display

Analog & Color-Graded Persistence	Variable saturation levels; stores each trace’s persistence data in memory.
Trace Selection	Activate Analog Persistence on a selected trace, top 2 traces, or all traces.
Persistence Aging Time	Select from 500 ms to infinity.
Trace Display	Opaque or transparent overlap
Sweeps Displayed	All accumulated or all accumulated with last trace highlighted

Zoom Expansion Traces

Display up to Four Zoom Traces	
	Vertical zoom up to 5X expansion, 50X with averaging
	Horizontal zoom expand to 2 pts/div, magnify to 50000X
	Auto Scroll automatically scans and displays any zoom or math trace.

Rapid Signal Processing

Processor	PowerPC
Processing Memory	Up to 128 Mbytes
Realtime Clock	Dates, hours, minutes, seconds and time stamp trigger time to 1 ns resolution

Internal Waveform Memory

Waveform	M1, M2, M3, M4 (Store full-length waveforms with 16 bits/data point)
Zoom and Math	Four traces A, B, C, D with chained trace capability

Setup Storage

Front Panel and Instrument Status	Four non-volatile memories and floppy drive are standard. Hard drive and memory card are optional.

Interface

Remote Control	Full control of all front panel controls and internal functions via RS232C, GPIB, or Ethernet
RS-232-C	Asynchronous transfer rate of up to 115.2 kbaud
GPIB Port	Full control via IEEE – 4888.2; configurable as talker/listener for computer control and data transfer
Ethernet (optional)	10 BaseT Ethernet interface
Floppy Drive	Internal, DOS-format, 3.5" high-density
PC Card Slot (optional)	Supports memory and hard drive cards
External Monitor Port Standard	15-pin D-Type VGA-compatible
Centronics Port	Parallel printer interface
Internal	Provides hard copy output in <10 seconds

Graphics Printer (optional)

Outputs

Calibrator Signal	500 Hz – 1 MHz square wave or DC level; select from -1.0 to +1.0 Volt into 1 MOhms output on front panel test point and ground lug.
Control Signals	Rear Panel, TTL level BNC output; Choice of trigger ready, trigger out, pass/fail status. (output resistance 300 Ohms +- 10%)

Environmental and Safety

Operating Conditions	
Temperature	5 – 40 °C rated accuracy 0 – 45 °C operating -20 – 60 °C non-operating
Humidity	80% max RH, non-condensing at 35 °C; Derates to 50% max RH, non-condensing at 45 °C
Altitude	4500 meters (15 000 feet) max. up to 25 °C; Derates to 2000 meters (6600 feet) at 45°C
CE Approved	
EMC	EMC Directive 89/336/EEC; EN 61326-1 Emissions and Immunity
Safety	Low Voltage Directive 73/23/EEC; EN 61010-1 Product Safety (Installation Category II, Pollution Degree 2)
UL and cUL approved	UL Standard UL 3111-1 cUL Standard CSA-C22.2 No. 1010-1

From www.lecroy.com

HELIUM-NEON LASER

Manufacturer	Melles Griot
Model	05-LLR-851 (Specs from similar Class IIIb laser)
Output wavelength	633 nm
Output Power	10 mW
Transverse Mode	TEM_{00}
Longitudinal Mode Spacing	341 MHz
M_2	<1.05
Beam Dimension ($1/e^2$)	0.65 mm
Far-Field Divergence ($1/e^2$)	1.24 mrad
Polarization	Linear, >500:1
Angular Drift	<0.03 mrad after 15 min
Noise (rms)	<5% (30 Hz to 10 MHz)
Bore-Sight Error	<0.1 mrad
Maximum Mode Sweeping	2%
Long-Term Drift	±2%
Operating Temperature	−20°C to +40°C
Nonoperating Temperature	−40°C to +80°C
Operating Humidity	0–90%
Nonoperating Humidity	0–100%
CDRH Class	IIIb
IEC Class	3B

From www.mellesgriot.com

SILICON OPTICAL SENSOR

Model	**818-SL**
Spectral Range (m)	0.4–1.1
Power, Average Max w/ Attenuator (W/cm^2)[1]	2
Power, Average Maximum w/o Attenuator (mW/cm^2)[1]	2
Pulse Energy, Maximum - w/ Attenuator (J/cm^2)[2]	1
Pulse Energy, Maximum - w/o Attenuator (nJ/cm^2)[2]	1
Accuracy at constant temperature[8]	±2% @ 0.4-1.1 m[5]
Uniformity (%)[6]	±2
Linearity (%)	±0.5
Saturation Current (mA/cm^2)	4.6
Responsivity	>0.1 A/W 400–1000 nm
Responsivity (Peak)	>0.5 A/W @ 400–1000 nm
Material	Silicon
Active Area (cm^2)	1
Active Diameter (cm)	1.13
Shape	Cylinder

THIS PAGE INTENTIONALLY LEFT BLANK

APPENDIX B. MATLAB SIGNAL PROCESSING CODE

The following code was used to evaluate the input signal and fuel injection pulse signal.

```
clear all
clc;

injector = input('Please enter injector# [1-4]: ','s');
pressure = input('Please enter test pressure in psi [500-2000]: ','s');
runnumber = input('Please enter Run Number [0-3]: ','s');
file1 = ['I' injector '.' pressure '.SC1.00' runnumber];
file2 = ['I' injector '.' pressure '.SC2.00' runnumber];
fprintf('File1 = %s and File2 = %s\n',file1,file2);
correct = input('Are these the correct filenames? [Y/N]: ','s');
if (correct == 'n') & (correct == 'N')
   file1 = input('Please enter correct filename #1: ');
   file2 = input('Please enter correct filename #1: ');
end;

CH1=LCREAD(file1);
CH2=LCREAD(file2);
CH1.x=CH1.x*1000;
CH2.x=CH2.x*1000;
CH1.y=0.1*CH1.y;
CH2.y=-1*CH2.y;

plot(CH1.x, CH1.y, CH2.x, CH2.y);
xlabel('Time (ms)');
ylabel('Volts');
hold;
plot([0 200],[1 1],'k');

fprintf('\nPress any key to continue...\n\n');
pause;

j=1;
i=1;
k=1:10;
delay1(k)=0;
width1(k)=0;
delay2(k)=0;
width2(k)=0;
delay(k)=0;
width(k)=0;
while j<11
```

```
    while CH1.y(i) < 1
        i=i+1;
    end;
    delay1(j) = CH1.x(i);
    i=i+1;
    while CH2.y(i) > 1.0
        i=i+1;
    end;
    delay2(j) = CH2.x(i);
    i=i+1;
    while CH2.y(i) <= 1.05
        i=i+1;
    end;
    width2(j) = CH2.x(i);
    while CH1.y(i) > 1
        i=i+1;
    end;
    width1(j) = CH1.x(i);
    i=i+10;
    j=j+1;
end;

fprintf('Shot# \t Delay (ms) \t Width (ms)\n');
k=1;
while k<11
    delay(k) = delay2(k) - delay1(k);
    width(k) = width2(k) - delay2(k);
    fprintf('%i \t \t %6.3f \t \t %6.3f\n', k, delay(k), width(k) );
    k=k+1;
end;
```

APPENDIX C. INDIVIDUAL INJECTOR PULSE CHARACTERISTICS

Single pulse characteristics for each injector for pressures between 750 psi and 1500 psi are shown below.

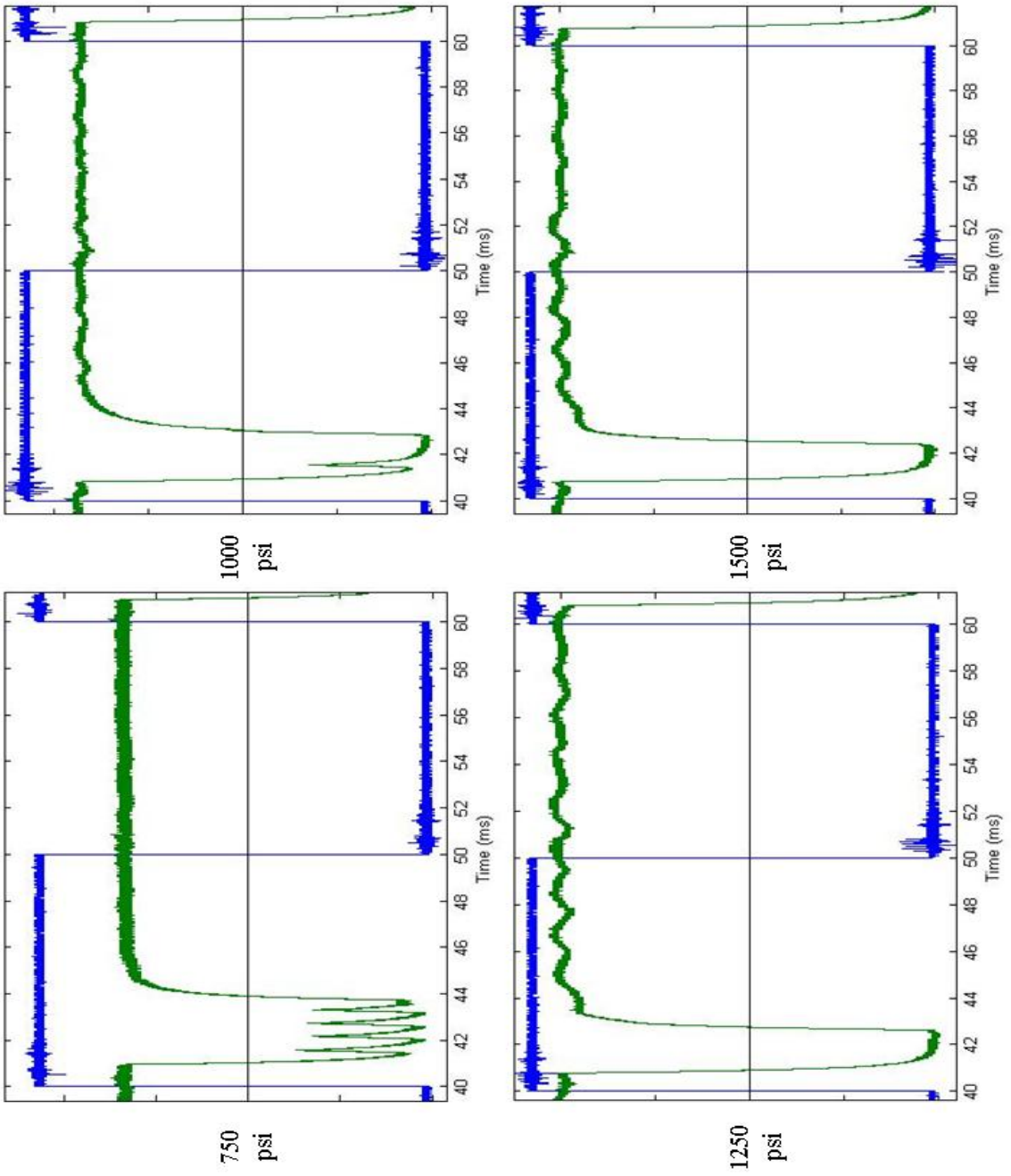

Figure 26. Typical pulses for Injector 1 at various pressures

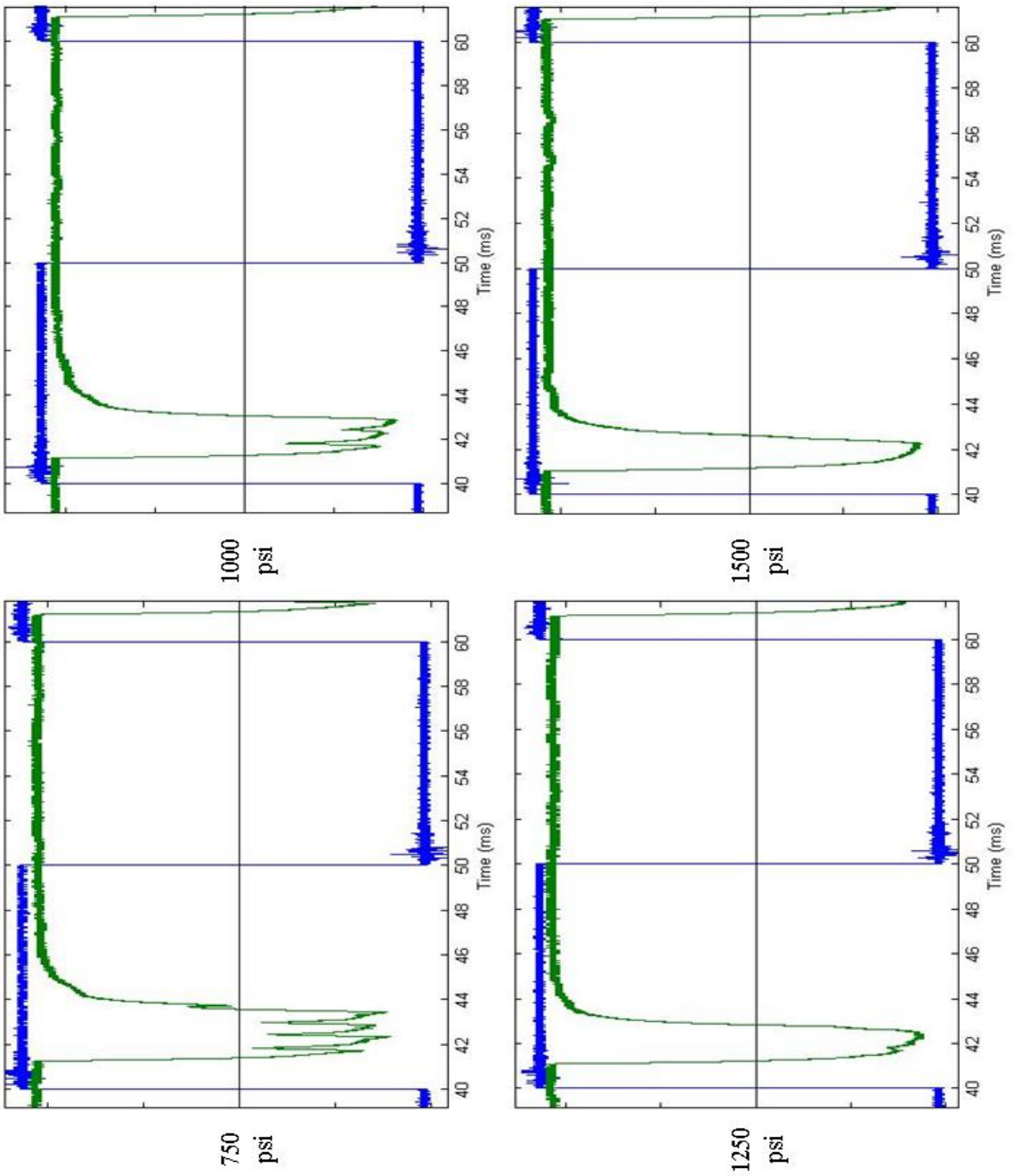

Figure 27. Typical pulses for Injector 2 at various pressures

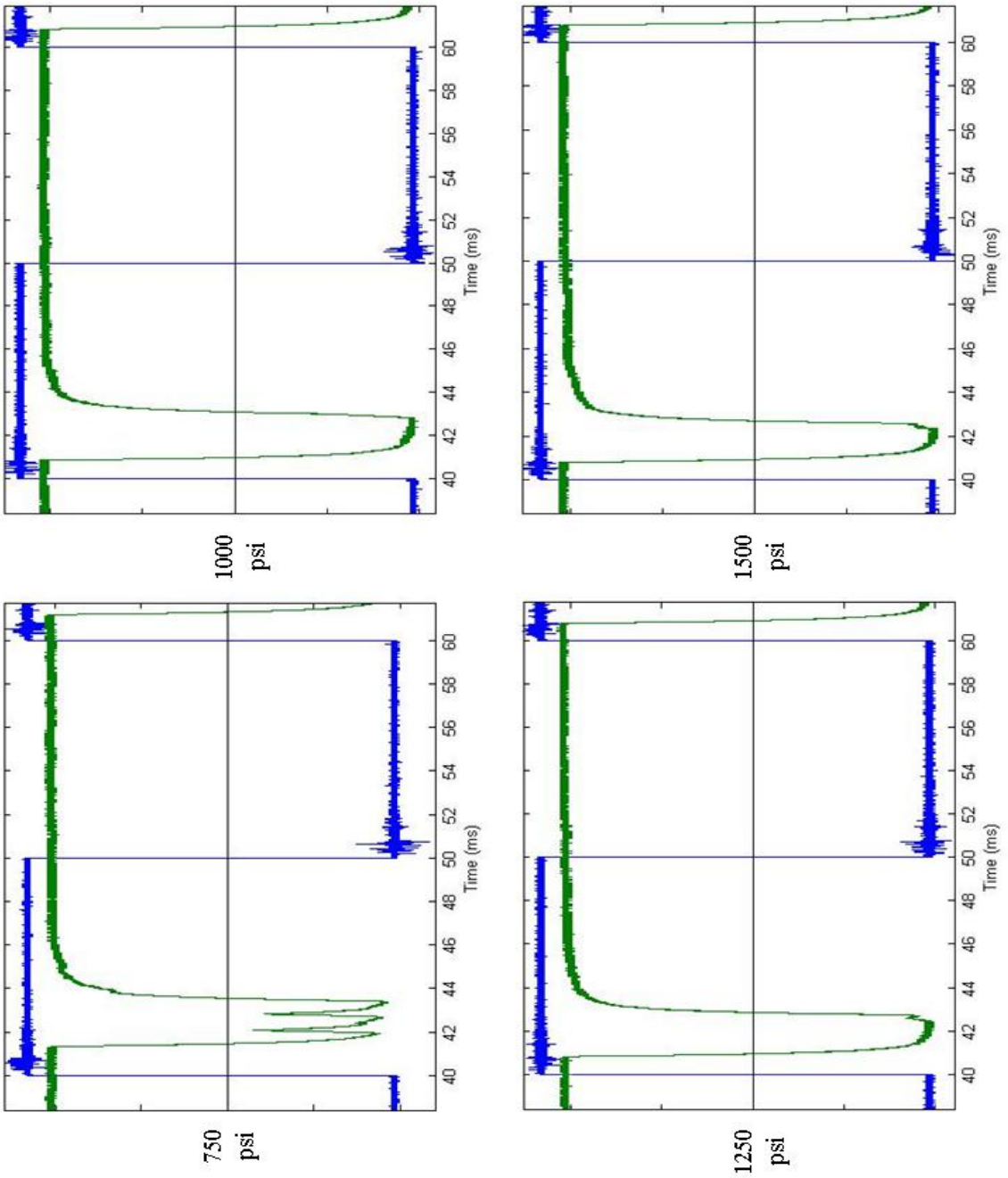

Figure 28. Typical pulses for Injector 3 at various pressures

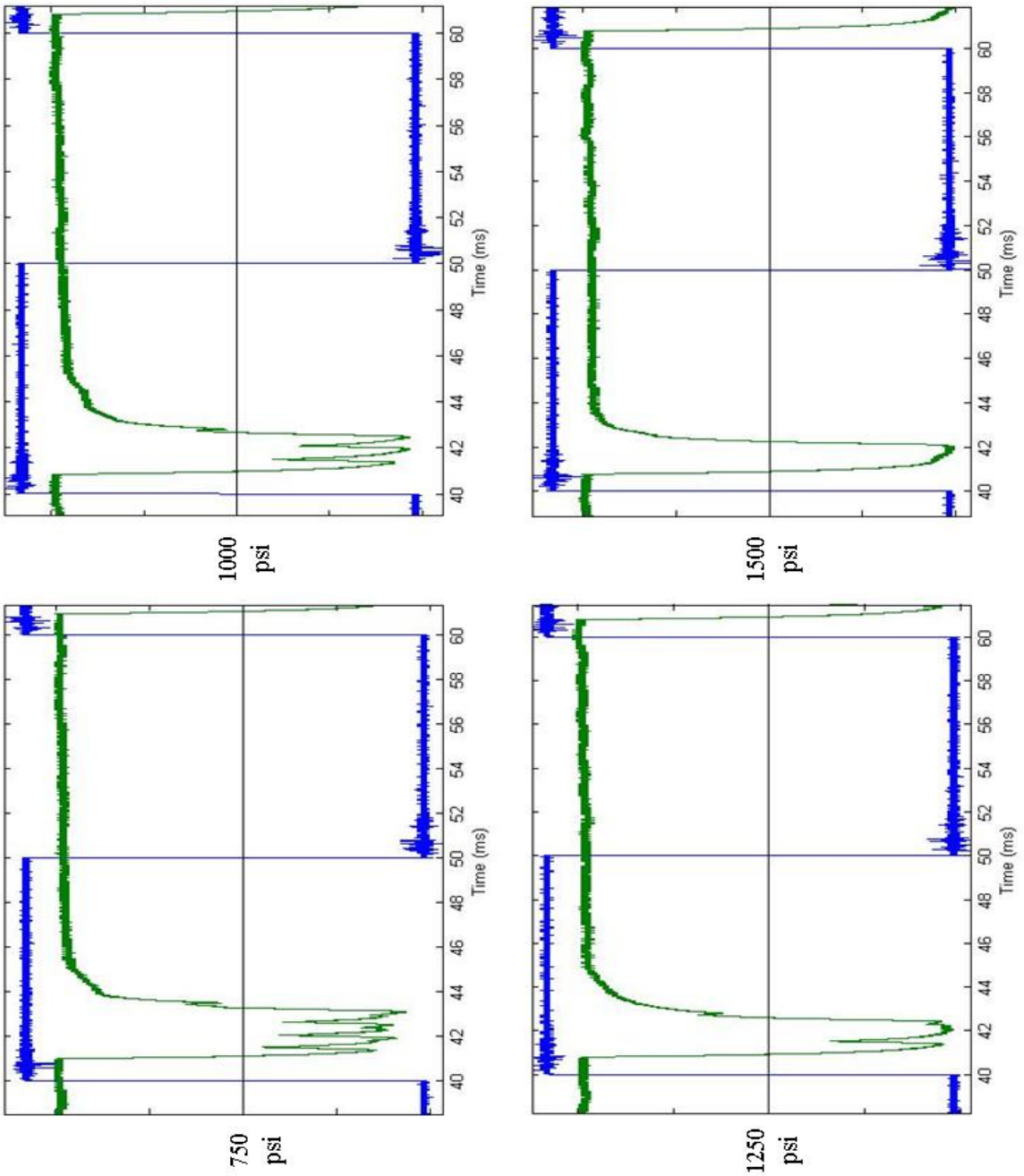

Figure 29. Typical pulses for Injector 4 at various pressures

APPENDIX D. ENGINEERING DRAWINGS

The engineering drawings for all complex components are shown below.

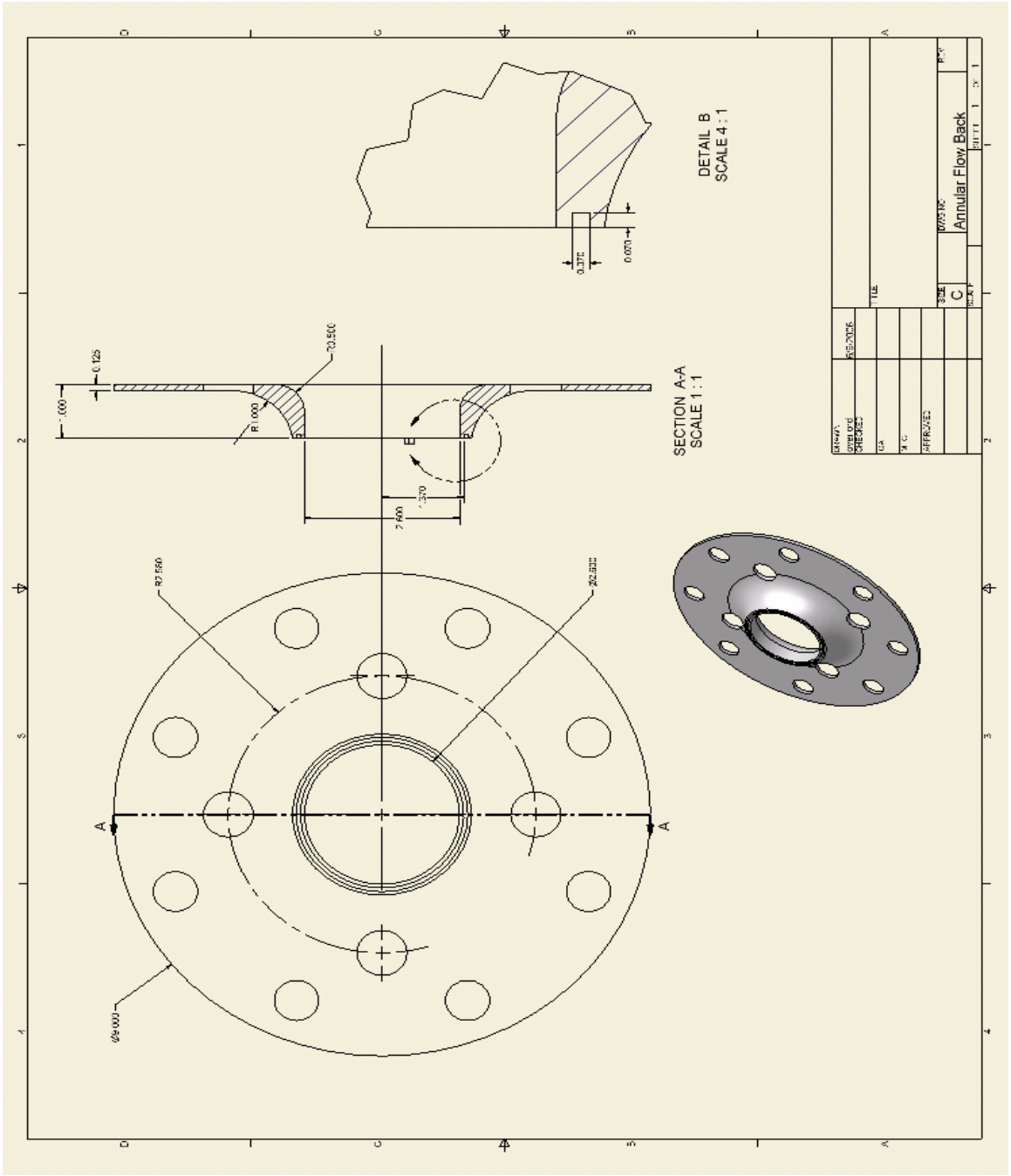

Figure 30. Machine drawing – Outer flow turning flange backing plate

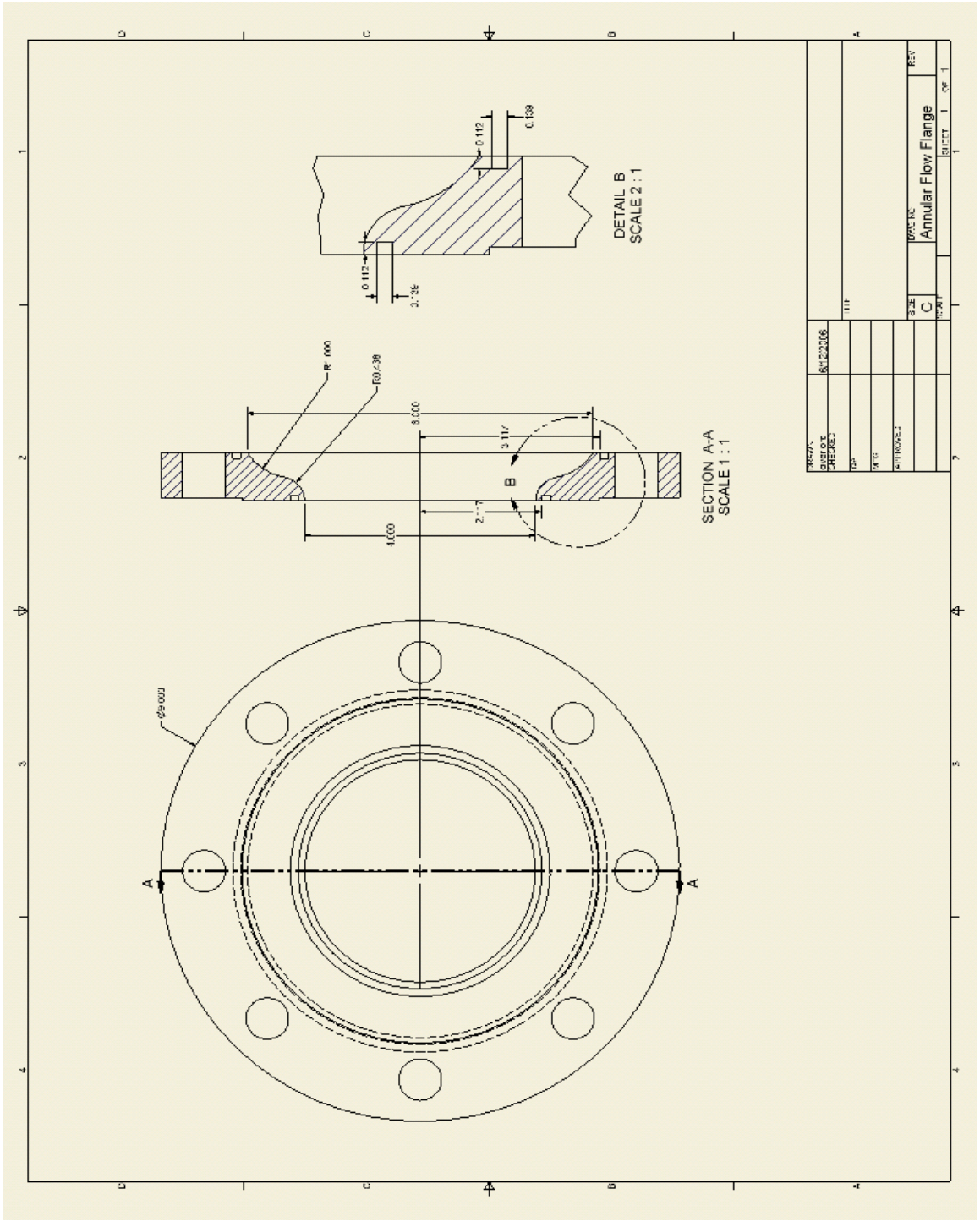

Figure 31. Machine drawing – Outer flow turning flange

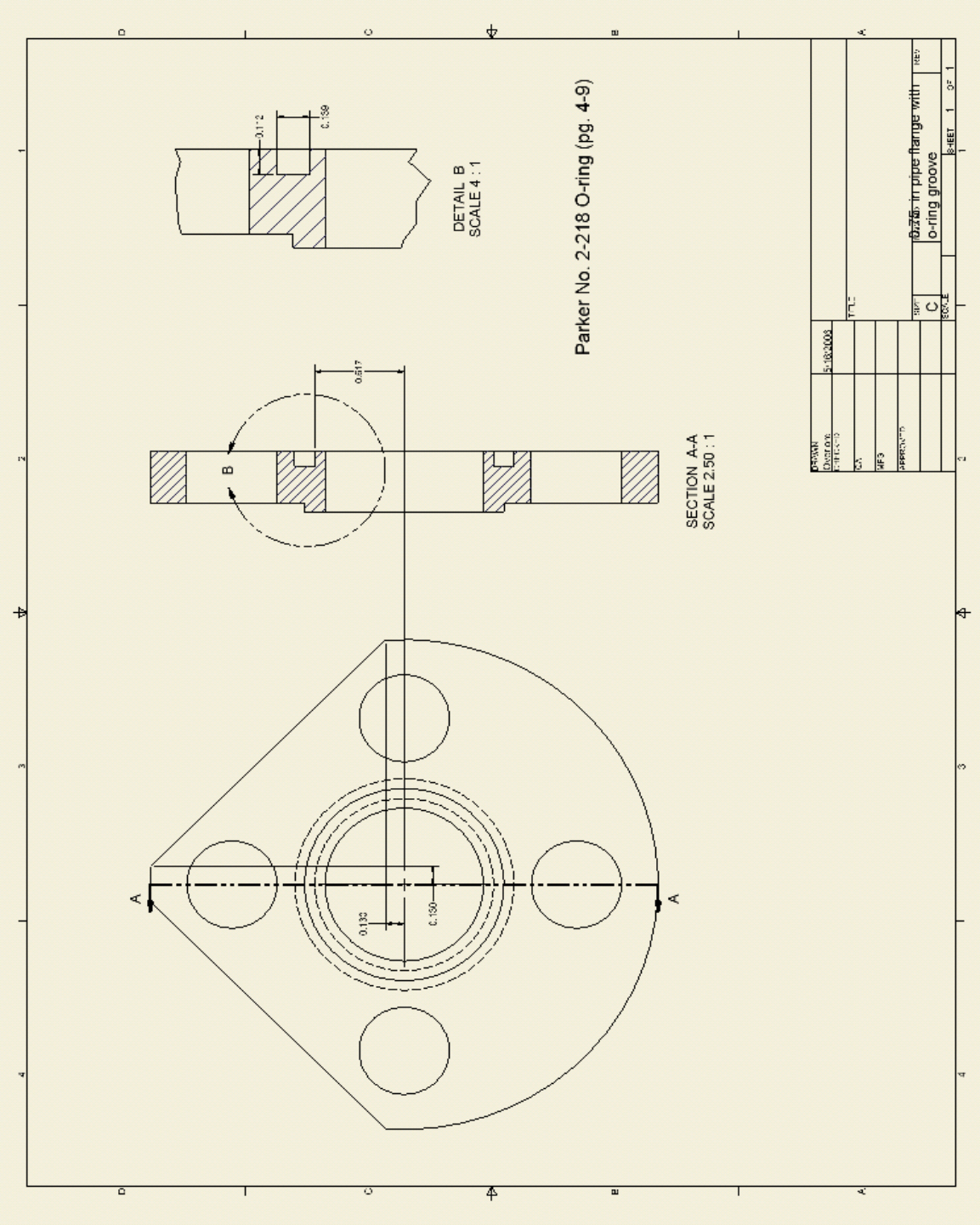

Figure 32. Machine drawing – Outer pipe flange

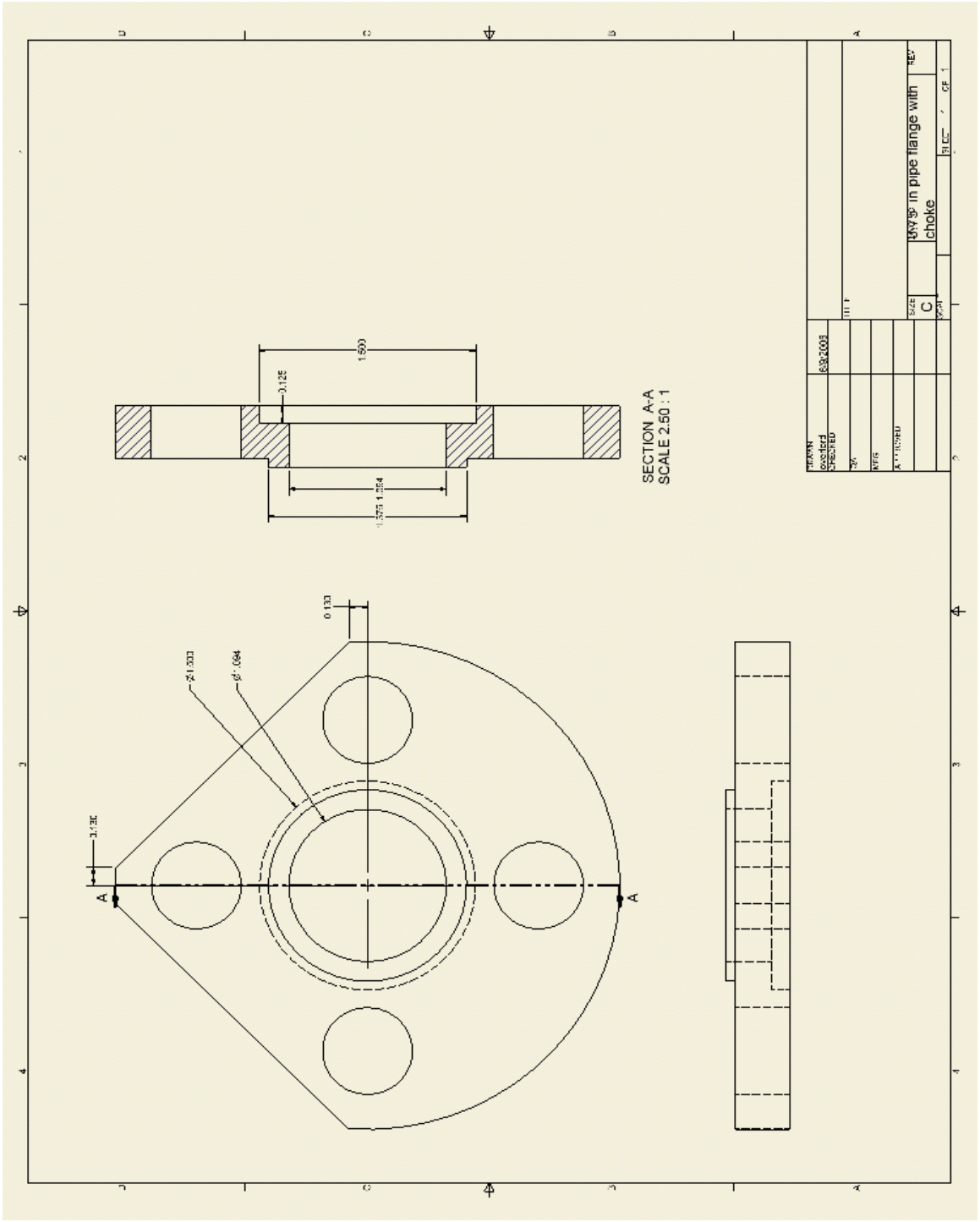

Figure 33. Machine drawing – Outer pipe flange with choke recess

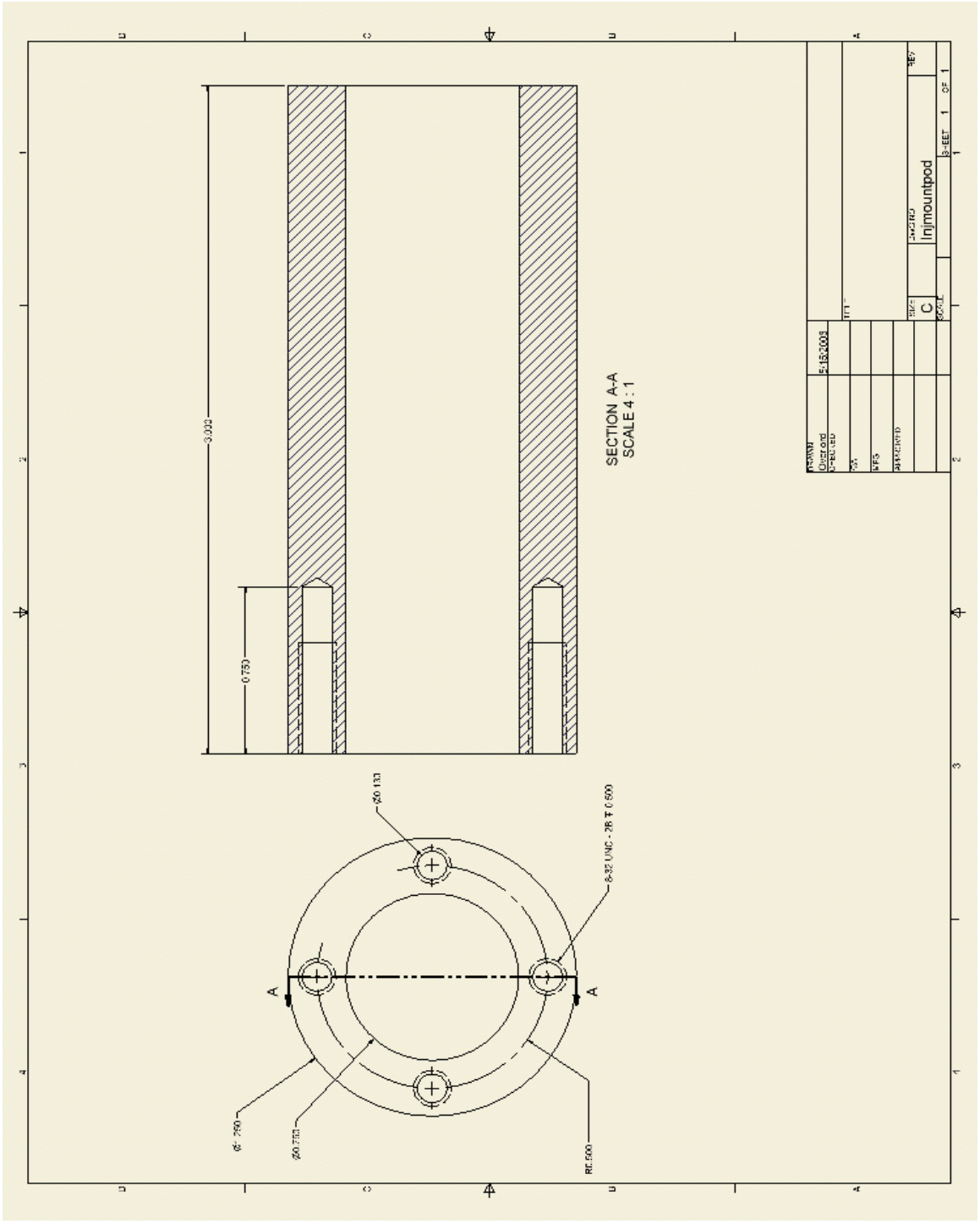

Figure 34. Machine drawing – Fuel injector mount

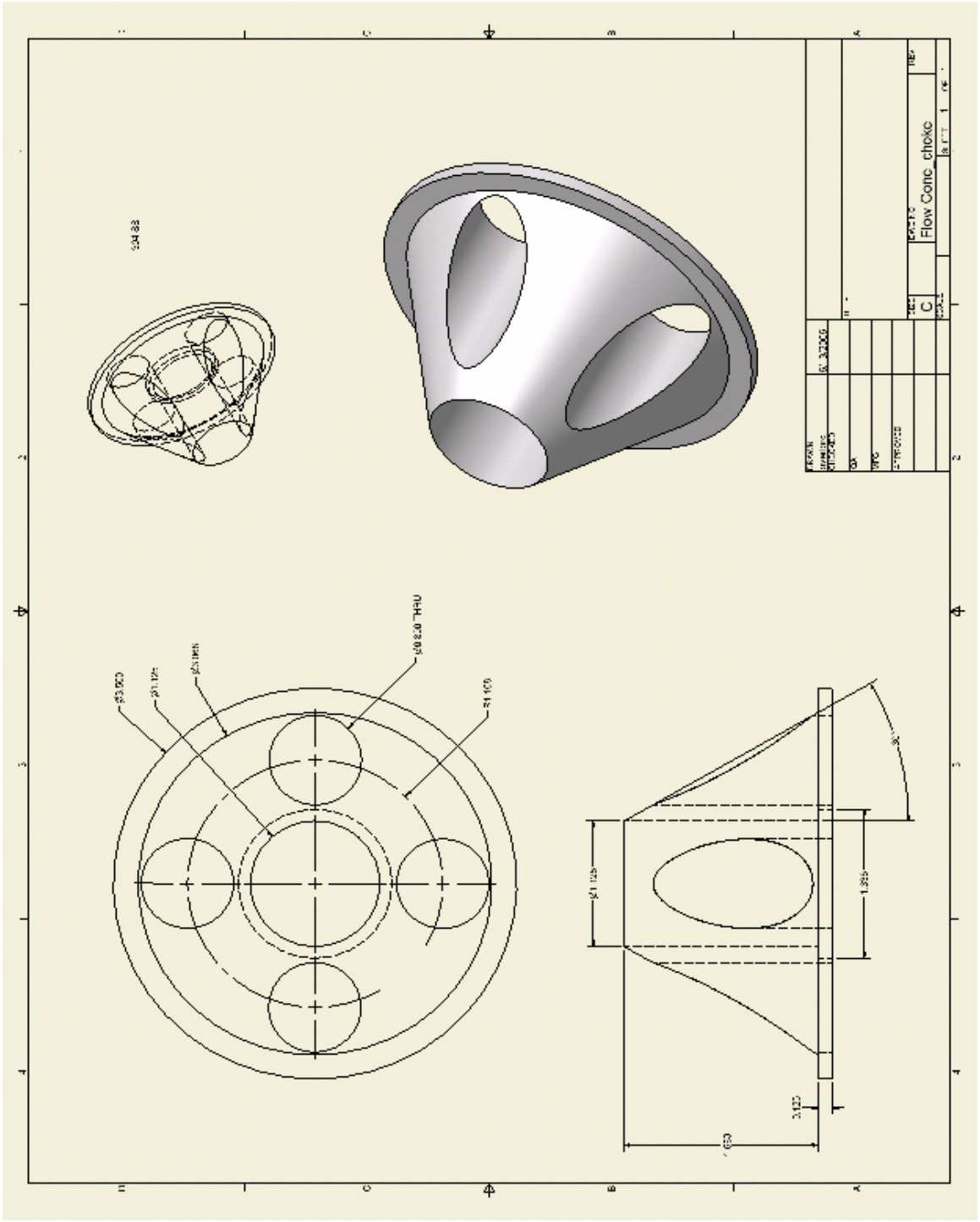

Figure 35. Machine drawing – Flow split cone

LIST OF REFERENCES

1. Hall, P., "Design of a Coaxial Split Flow Pulse Detonation Engine," Master's Thesis, Naval Postgraduate School, Monterey, California, June 2006.

2. Gundersen, M., "Transient Plasma Ignition – Non-Thermal Plasma Actuator," http://www.usc.edu/dept/ee/Gundersen/ignition.htm#Transient, May 2006.

3. Holthaus, J., "Computational Investigation of the Internal Flow Path and Wave Dynamics of Pulse Detonation Engine Operation," Master's Thesis, Naval Postgraduate School, Monterey, California, June 2006.

4. Hutcheson, P., Holthaus, J., Brophy, C., and Sinibaldi, J., "Design and Performance Testing of a Split-path JP-10/Air Pulse Detonation Engine," AIAA Paper, *Joint Propulsion Conference and Exhibit*, Sacramento, California, 9-12 July 2006.

5. Hoffman, H., "Reaction-Propulsion Produced by Intermittent Detonative Combustion," German Research Institute for Gliding, Report ATI-52365, August 1940.

6. Damphouse, P., "Characterization and Performance of a Liquid Hydrocarbon-Fueled Pulse Detonation Rocket Engine," Master's Thesis, Naval Postgraduate School, Monterey, California, December 2001.

7. Kuo, K.K., *Principles of Combustion*, Second Edition, John Wiley and Sons, 2005.

8. Rodriguez, J., "Investigation of Transient Plasma Ignition for a Pulse Detonation Engine," Master's Thesis, Naval Postgraduate School, Monterey, California, March 2005.

9. Bussing, T., and Pappas, G., "An Introduction to Pulse Detonation Engines," AIAA Paper 1994-0263, 32nd AIAA Aerospace Sciences Meeting and Exhibit, Reno, Nevada, 10-13 January 1994.

10. Hartsfield, C., "Reactive Shear Layer Mixing and Growth Rate Effects on Afterburning Properties for Axisymetric Rocket Engine Plumes," Doctoral Dissertation, Naval Postgraduate School, Monterey, California, December 2005.

11. Whittmers, N., "Direct-connect Performance Evaluation of a Valveless Pulse Detonation Engine," Master's Thesis, Naval Postgraduate School, Monterey, California, December 2004.

THIS PAGE INTENTIONALLY LEFT BLANK

INITIAL DISTRIBUTION LIST

1. Defense Technical Information Center
   Ft. Belvoir, Virginia

2. Dudley Knox Library
   Naval Postgraduate School
   Monterey, California

3. Jose O. Sinibaldi
   Naval Postgraduate School
   Monterey, California

4. Christopher M. Brophy
   Naval Postgraduate School
   Monterey, California

5. Ashok Gopinath
   Naval Postgraduate School
   Monterey, California

6. Tad J. Robbins
   Naval Postgraduate School
   Monterey, California